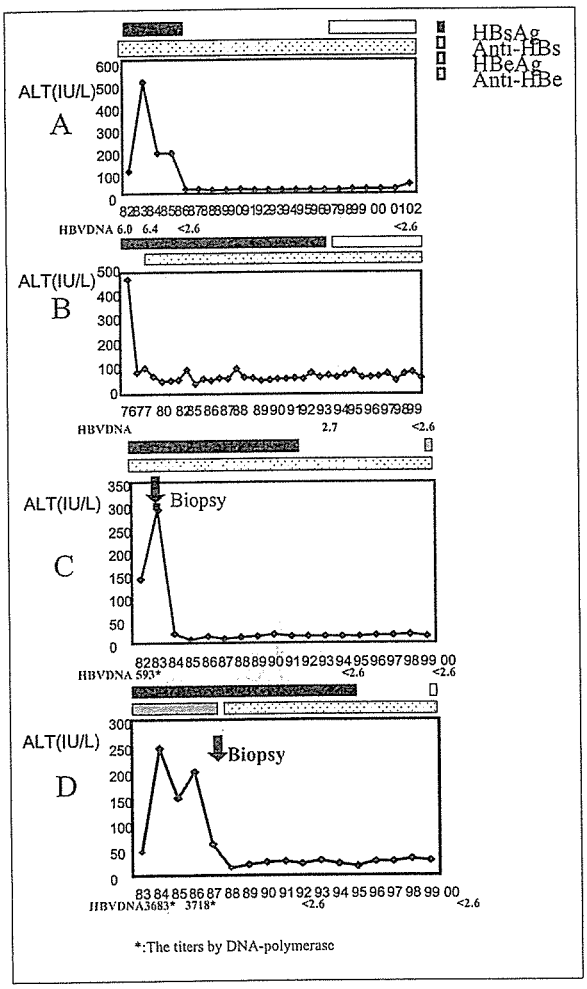

FIGURE 1 The clinical course and the HBV markers in the 4 patients. HBV DNA titers were detected by amplicore monitor assay (log copy/mL) (Roche), except for those at the early periods of patient C and D, which were expressed by DNA polymerase (cpm/mL).

METHODOLOGY AND RESULTS

Patient A had been followed for chronic hepatitis B since 1982 when he was 55 years old **(Figure 1)**. Liver biopsy in 1983 revealed precirrosis **(Figure 3, A-a)** with active inflammation [A3 (13)] **(Figure 2A)**. As active HBV replication naturally ceased and ALT values had normalized in 1985. They continued to be normal thereafter. HBsAg became negative in 1986 and anti-HBs became positive in 1998. Ultrasonography pointed out liver tumor in 2002. HCC was confirmed by computerized tomography (CT), magnetic resonance imaging (MRI) and a specific increase of PIVKA (Protein Induced by Vitamin K Absence or antagonist) II (45300mIU/mL). A biopsy from non-tumor liver that was performed after informed consent, showed almost no fibrosis **(Figure 3, A-c)**. The patient died with rapid progression of tumor and an autopsy was performed. Non-HCC part of liver showed only thin fibrous septa with no inflammation **(Figure 3, A-b)**.

In patient B liver injury was pointed out in 1974 when he was 32 years old. He had a severe liver injury and was diagnosed with subacute viral hepatitis. He once had recovered from severe stage of hepatitis, but chronic active hepatitis B (positive for HBeAg) continued. Histology of liver showed severe inflammation (A3) **(Figure 2B)** with some regenerative nodules in 1979 **(Figure 3, B-a)**. Seroconversion from HBeAg to anti-HBe occurred in 1986. The ALT values had decreased since then. HBsAg became negative in 1998 and anti-HBs became positive at the same time. Solitary HCC was pointed out in the S6 region in 1999 and it was resected in 1999. Non-HCC part of liver showed fibrous septa that might be in the absorbing stage, and there was almost no finding of active inflammation **(Figure 3, B-b)**.

Clinical course of patient C and D were already described in our previous paper (12). Briefly, patient C was a 79-year-old male when solitary HCC was resected in 2000. He had been followed in our hospital since 1979 for chronic hepatitis B. A liver biopsy in 1983 revealed extensive portal fibrosis (precirrhosis) **(Figure 3, C-a)** and active inflammation (A2) **(Figure 2C)**. His disease activity naturally resolved and he had had a normal level of ALT values for 16 years until the diagnosis of HCC was made. He has been negative for HBsAg since 1993 and anti-HBs was positive when HCC was diagnosed. Non-HCC part of liver also showed only thin scarred fibrous septa with no inflammation **(Figure 3, C-b)**. Patient D had been followed for active chronic hepatitis B and diagnosed with active liver cirrhosis by liver biopsy (A2) **(Figure 2D and Figure 3, D-a)** when he was 35 years old. The ALT values had been normalized since 1988. He has been negative for HBsAg since 1997. He was diagnosed with HCC by typical computerized tomography finding in 2000. Anti-HBs was found to be positive almost at the same time when the diagnosis of HCC was made.

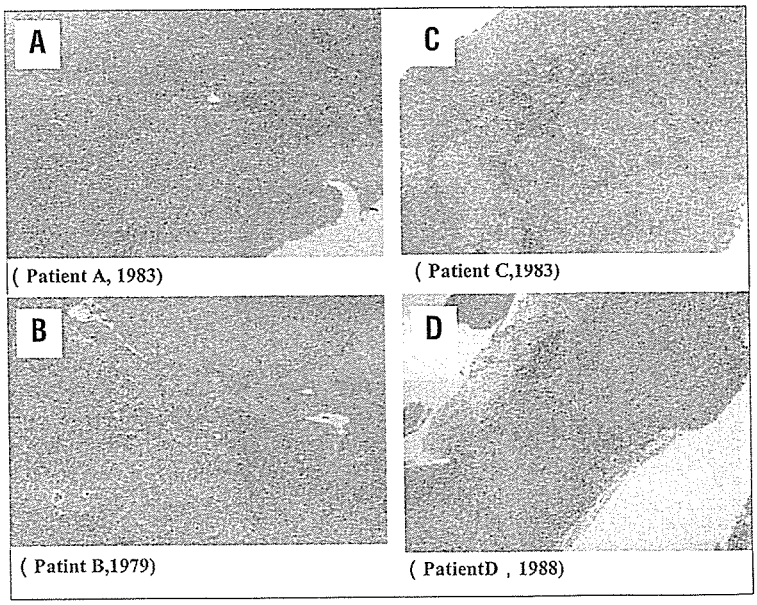

FIGURE 2 Hematoxylin and eosin staining of the liver tissues obtained when disease was active. (**A**: patient A in 1983, **B**: patient B in 1979, **C**: patient C in 1983, **D**: patient D in 1988). Magnification was x400.

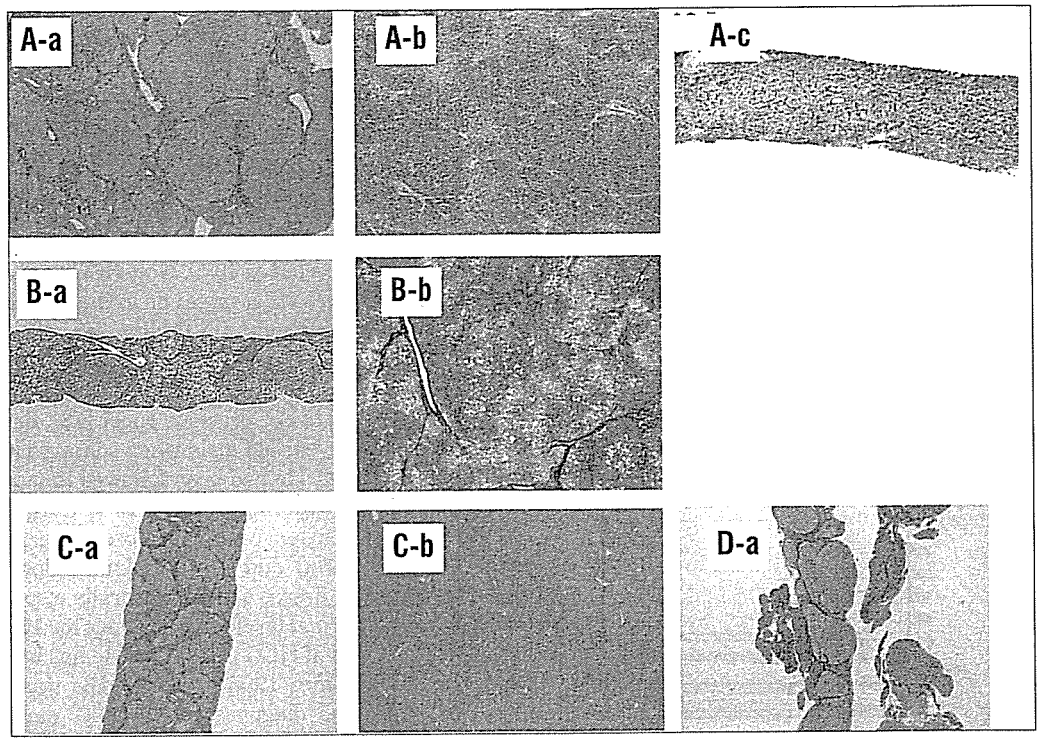

FIGURE 3
Changes of fibrosis levels of liver in the patients from the time when disease was active (**A-a**: patient A in 1983, **B-a**: patient B in 1979, **C-a**: patient C in 1983, **D-a**: patient D in 1988) to the time when HCC developed (**A-c**: patient A at biopsy and **A-b**: at autopsy each in 2002, **B-b**: patient B at surgery in 1999, **C-b**: patient C at surgery in 2000. Slides were silver stained. Liver tissue was not obtained from patient D when HCC developed. Silver staining was performed and the magnification was x125.

We retrospectively examined the HBV DNA titers of the stored serum samples of all the 4 patients, using amplicore monitor assay (Roche Diagnostics, Japan). The HBV DNA titers were less than the detection limit (<2.6 log copy/mL) in all of the sera obtained after the clinical remission, except the one obtained from patient B in 1993 that showed 2.7 log copy/mL (**Figure 1**). High titers of HBV DNA in the periods of active inflammation were confirmed in the stored sera in this patient. They were also confirmed in the clinical records by the values of HBV-DNA polymerase in the patient C and D, but not confirmed in the patient B because it was too long ago and the tests were not performed. Anti-HBc was positive for all the 4 patients when HCCs were diagnosed. It remained positive in the sera from patient B, C, and D, when diluted by 200 times, and became negative in patient A.

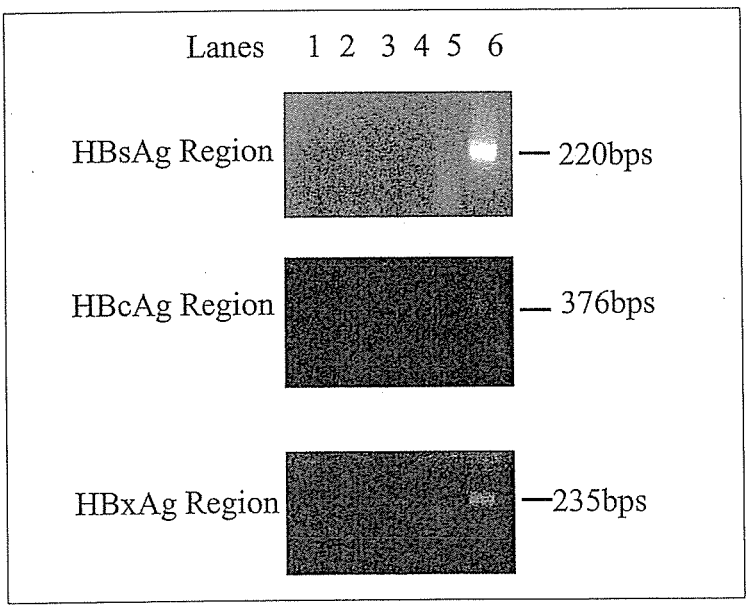

FIGURE 4 A result of nested PCR analysis for HBV DNA in the paraffin-embedded tissue obtained when the HCCs occurred. Autopsy specimen from patient A and surgically-resected specimen in each patient B and C, were analyzed. The PCR was performed for HBsAg region (Upper), HBcAg region (Middle) and HBxAg region, respectively. Lane 1, 2 and 6 shows the result from the buffer, HBsAg-negative, and positive paraffin-embedded tissue, respectively. Lane 3, 4 and 5 show the result from patient A, B and C, respectively.

HBV DNA was examined for liver tissues obtained at surgery in patient B and C, and at autopsy in patient A, by PCR analysis. Paraffin-embedded tissues in which the major part was HCC tissue were cut in slices 5μm thick, treated with xylene twice and followed by 100, 95 and 70% ethanol gradient. Tissues were treated with 20μg/mL of proteinase K (Sigma, St. Lois, MO) in 10mM Tris (8.0), 150mM NaCl, 0.1% of Sodium Dodecyl Sulfate at 55°C overnight. After phenol and chroloform extraction, DNA was precipitated by ethanol. DNA was dissolved in 10mM Tris (8.0), 1mM EDTA.

A part of the surface, core, and x region of the HBV genome was amplified by a nested polymerase chain reaction using 1μL of resuspended DNA in a final volume of 25μL containing 0.3mM dNTP, 1μM of each sense and antisense external primers, and 0.6U Taq polymerase (Promega, Madison,WI). 1μL of first-round PCR product was subjected to second-round PCR using internal sense anti-sense primers. The external primers were as follows: 5'-GGGACCCTG-CACCGAACATG-3' [sense, nt 11 to 30 of HBV

genome (14)] and 5'-AGCAGGATGAAGAGGAATAT-3' (antisense, nt 271 to 290) for HBs region, 5'- ATGGAGACCACCGTGAACGC-3' (sense, nt 1480 to 1499) and 5'-GGCGAGGGAGTTCTTCTTCTAGGGG-3' (antisense, nt 2,236 to 2,260) for HBc region, 5'-GAACCTTTGTGGTTCCTCTG -3' [sense, (15)] and 5'- ATTGCTGAGAGTCCAAGAGTCC -3' (antisense) for HBx region. Primers for the second PCR were 5' CATCAGGATTCCTAGGACCC-3' (sense, nt 41 to 60) and 5'-CGCAGACACATCCAGCGATA-3' (antisense, nt 241 to 260) for HBs, 5'-AGGTCTTGCCCAAGGTCTTA-3' (sense nt 1505 to 1524) and 5'-AGCTGAGGCGGTGTCGAGGAGATC-3' (antisense, nt 1,857 to 1,880) for HBc, 5'-TCCTTTGTCTACGTCCCGTC-3' (sense) and 5'-TAAGAGCTTGGGCAAGACC -3' (antisense) for HBx region. 220 bps for HBs, 376 bps for HBc, and 235 bps for HBx were amplified. The reaction was performed in 35 cycles of 94°C for 1 minute, 55°C for 45 seconds, and 72°C for 1 minute. The PCR products were analyzed by 1.5% agarose gel **(Figure 4)**.

DISCUSSION

The four patients revealed very similar clinicopathological features that were considered to be very informative in the occurrence of HCC due to chronic HBV infection. Although this is the report of only 4 cases, these similar characteristic features can lead us to understand the general characteristics of the disease.

First, all the patients had established precirrhosis or cirrhosis due to severe liver injury by active HBV replication more than a decade ago and delayed clearance of HBsAg occurred later. In our recent investigation for HBV carriers who have visited outpatient clinic of our and affiliated hospitals, 6 of 476 (1.2%) of HBV carriers had cleared of HBsAg at an average of 13 years since the first visit (unpublished data). Three of the 6 patients had been diagnosed with liver cirrhosis at the latest visit. Liver cirrhosis is one of the factors that affect the loss of HBsAg (3). Significant liver damage leading to precirrhosis or cirrhosis occurred when these patients were in the phase of active HBV replication. The occurrence of HCC may be closely associated with these precirrhotic or cirrhotic livers that have highly cancer-prone characteristic.

We had to use paraffin-embedded tissue to detect HBV sequences using PCR, because of an unavailability of frozen tissues. No apparent detection of HBV sequence in the tumor tissues by PCR for surface, core, and x region of HBV can have some implication of the role of HBV in the hepatocarcinogenesis of these patients. It is easily conceivable that the active replication of HBV in the liver might not have occurred for a long period, because of the undetectable HBV DNA in the sera by the sensitive tests. Another consideration is the integration of HBV into the genome of the hepatocyte that invariably occurs in patients with chronic HBV infection. The integrated HBV DNA has been shown to result in chromosomal rearrangement and deletion, and to be involved in hepatocarcinogenesis. Undetectable HBV DNA by the PCR analysis in the liver DNA also may deny the presence of integrated HBV sequence in the tumor. If so, the original tumor clone in these patients might not arise from the liver when HBV actively replicated, that is more than a decade previously, but rather originated from the liver where active replication of HBV almost ceased. However, these possibilities still remain speculative and Southern blot hybridization analysis for HBV DNA using frozen tissues to show replicative intermediate or integrated fragment of HBV is needed to clarify this issue.

In general, fibrosis level of liver that harbors HCC due to HBV is milder than that due to HCV (8-11). However, the decreased and improved fibrosis level in the background liver of the patients when HCC developed, compared to the previous fibrosis level, may shed light on the pathological aspect of HBV-induced HCC. Because chronic HBV infection naturally remits and inflammatory activity decreases in a majority of patients, we speculate that this improving and absorbing of fibrosis, the phenomenon of which is similar to that when HCV was eradicated with interferon (16), can usually occur in a large number of patients. And the dramatic improvement of fibrosis in the background liver of HCC led us to assume that some commonly-observed mild fibrosis levels in the liver of HBV-induced HCC may be the one that returns from high fibrosis level established when the inflammation due to HBV was active. A comparison of histology between the one obtained by a needle biopsy and the large one by autopsy (patient A, **Figure 2** and **3 A-b, and A-c**) also gives us a good suggestion in evaluating the level of fibrosis. Thin fibrous septa that has been in the process of absorption and surrounds a large nodule might not be recognized if the tissue is small, such as in our case by needle biopsy. Thus, unless we use large specimens obtained by surgical resection or autopsy, the precise evaluation of fibrosis level may be disturbed.

From these findings, we would again like to emphasize that in some patients with HBV HCC, the level of progression of the disease, in terms of fibrosis level, may be underestimated because we might see it when it is in the process of improving and being absorbed. We are extending this pathological evaluation to the past surgically-resected HBV HCC specimens in our facility and confirming that this thin-fibrous-septa pattern without active inflammation exists in a relative majority of patients in conjunction with classical liver cirrhosis patients (unpublished data). Those patients may have experienced once-progressed fibrosis like the patients reported in this study. Thus, actively intervening the inflammation caused by replication of HBV by anti-viral treatment to prevent the establishment of cirrhosis can be worthwhile, decreasing the incidence of hepatocarcinogenesis due to chronic HBV infection.

REFERENCES

1 **Sampliner RE, Hamilton FA, Iseri OA, Tabor E, Boitnott J:** The liver histology and frequency of clearance of the hepatitis B surface antigen (HBsAg) in chronic carriers. Am J Med Sci 1979; 277:17-22.

2 **Alward WLM, McMahon BJ, Hall DB, Heyward WL, Franchis DP, Bender TR:** The long-term serological course of asymptomatic hepatitis B virus carriers and the development of primary hepatocellular carcinoma. J Infect Dis 1985; 151:604-691.

3 **Liaw Y-F, Sheen I-S, Chen T-J, Chu C-M, Pao C-C:** Incidence, determinants and significance of delayed clearance of serum HBsAg in chronic hepatitis B virus infection: A prospective study. Hepatology 1991; 13:627-631.

4 **Liaw YF, Chen YC, Sheen IS:** Spontaneous clearance of hepatitis B surface antigen in chronic hepatitis B virus infection confers a favorable response. Hepatology 1999; 29:296.

5 **Perrillo RP, Brunt EM:** Hepatic histologic and immunohistochemical changes in chronic hepatitis B after prolonged clearance of hepatitis B e antigen and hepatitis B surface antigen. Ann Intern Med 1991; 115:113-115.

6 **Huo TI, Wu JC, Lee PC, Chau GY, Lui WY, Tsay SH, Ting LT, Chang FY, Lee SD:** Sero-clearance of hepatitis B surface antigen in chronic carriers dose not necessarily imply a good prognosis. Hepatology 1998; 28:231-236.

7 **McMahon BJ:** Chronic carriers of hepatitis B virus who clear hepatitis B surface antigen: Are they really "Off the hook". Hepatology 1998; 28:265-267.

8 **Shiratori Y, Shiina S, Imamura M, et al:** Characteristic difference of hepatocellular carcinoma between hepatitis B and C viral infection in Japan. Hepatology 1995; 22:1027-1033.

9 **Miyagawa S, Kawasaki S, Makuuchi M:** Comparison of the characteristics of hepatocellular carcinoma between hepatitis B and C viral infection: tumor multicentricity in cirrhotic liver with hepatitis C. Hepatology 1996; 11:944-948.

10 **Sato A, Kato Y, Nakata K, et al:** Relationship between sustained elevation of serum alanine aminotransferase and progression from cirrhosis to hepatocellular carcinoma: comparison in patients with hepatitis B virus- and hepatitis C virus associated cirrhosis. J Gastroenterol Hepatol 1996; 11:944-948.

11 **Shuto T, Hirohashi K, Kubo S, et al:** Difference of resected hepatocellular carcinoma with hepatitis B or C virus. Hepatogastroenterology 1998; 45:1722-1725.

12 **Okoshi S, Igarashi M, Suda T, Iwamatsu H, Watanabe K, Ishihara K, Ogata N, Nomoto M, Takahashi T, Ichida T, Asakura H, Nihei K, Kurosaki I:** Remote development of hepatocellular carcinoma in patients with liver cirrhosis type B serologically cured for HBs antigenemia with long-standing normalization of ALT values. Dig Dis Sci 2002 47:2002-2006.

13 **Scheuer PJ:** Classification of chronic viral hepatitis: a need for reassessment. J Hepatol 1991; 13:372-374.

14 **Fujiyama A, Miyanohara A, Nozaki C, Yoneyama T, Ohtomo N, Matsubara K:** Cloning and structural analysis of hepatitis B virus DNAs, subtype adr. Nucleic Acids Res 1982; 11:4601-4609.

15 **Katsuro K, Kobayashi M, Gondo M, Hayashi I, Osuga T, Takada S:** Hepatitis B virus DNA is frequently found in liver biopsy samples from hepatitis C virus-infected chronic hepatitis patients. J Med Virol 1998; 54:249-255.

16 **Shiratori Y, Imazeki F, Moriyama M, Yano M, Arakawa Y, Yokosuka O, Kuroki T, Nishiguchi S, Sata M, Yamada G, Fujiyama S, Yoshida H, Omata M:** Histologic improvement of fibrosis in patients with hepatitis C who have sustained response to interferon therapy. Ann Int Med 2000; 132:517-524.

Role of IP-10/CXCL10 in the progression of pancreatitis-like injury in mice after murine retroviral infection

Yusuke Kawauchi, Kenji Suzuki, Shiro Watanabe, Satoshi Yamagiwa, Hiroyuki Yoneyama, Gi Dong Han, Suresh S. Palaniyandi, Punniyakoti T. Veeraveedu, Kenichi Watanabe, Hiroshi Kawachi, Yoshiaki Okada, Fujio Shimizu, Hitoshi Asakura, Yutaka Aoyagi and Shosaku Narumi

Am J Physiol Gastrointest Liver Physiol 291:345-354, 2006. doi:10.1152/ajpgi.00002.2006

AJP - Gastrointestinal and Liver Physiology publishes original articles pertaining to all aspects of research involving normal or abnormal function of the gastrointestinal tract, hepatobiliary system, and pancreas. It is published 12 times a year (monthly) by the American Physiological Society, 9650 Rockville Pike, Bethesda MD 20814-3991. Copyright © 2005 by the American Physiological Society. ISSN: 0193-1857, ESSN: 1522-1547. Visit our website at http://www.the-aps.org/.

Am J Physiol Gastrointest Liver Physiol 291: G345–G354, 2006;
doi:10.1152/ajpgi.00002.2006.

Role of IP-10/CXCL10 in the progression of pancreatitis-like injury in mice after murine retroviral infection

Yusuke Kawauchi,[1] Kenji Suzuki,[1] Shiro Watanabe,[1] Satoshi Yamagiwa,[1] Hiroyuki Yoneyama,[2] Gi Dong Han,[3,6] Suresh S. Palaniyandi,[4] Punniyakoti T. Veeraveedu,[4] Kenichi Watanabe,[4] Hiroshi Kawachi,[3] Yoshiaki Okada,[5] Fujio Shimizu,[3] Hitoshi Asakura,[1] Yutaka Aoyagi,[1] and Shosaku Narumi[2]

Departments of [1]Gastroenterology and Hepatology and [3]Cell Biology, Institute of Nephrology, Niigata University Graduate School of Medical and Dental Sciences, Niigata; [5]Department of Bacterial and Blood Products, National Institute of Infectious Diseases, Tokyo; [2]Department of Molecular Preventive Medicine, University of Tokyo Graduate School of Medicine, Tokyo; [4]Department of Clinical Pharmacology, Niigata University of Pharmacy and Applied Life Sciences, Niigata, Japan; and [6]Department of Food Science and Technology, Yeungnam University, Gyeongsan, Republic of Korea

Submitted 4 January 2006; accepted in final form 1 April 2006

Kawauchi, Yusuke, Kenji Suzuki, Shiro Watanabe, Satoshi Yamagiwa, Hiroyuki Yoneyama, Gi Dong Han, Suresh S. Palaniyandi, Punniyakoti T. Veeraveedu, Kenichi Watanabe, Hiroshi Kawachi, Yoshiaki Okada, Fujio Shimizu, Hitoshi Asakura, Yutaka Aoyagi, and Shosaku Narumi. Role of IP-10/CXCL10 in the progression of pancreatitis-like injury in mice after murine retroviral infection. *Am J Physiol Gastrointest Liver Physiol* 291: G345–G354, 2006; doi:10.1152/ajpgi.00002.2006.—Exocrinopathy and pancreatitis-like injury were developed in C57BL/6 (B6) mice infected with LP-BM5 murine leukemia virus, which is known to induce murine acquired immunodeficiency syndrome (MAIDS). The role of chemokines, especially CXCL10/interferon (IFN)-γ-inducible protein 10 (IP-10), a chemokine to attract $CXCR3^+$ T helper 1-type $CD4^+$ T cells, has not been investigated thoroughly in the pathogenesis of pancreatitis. B6 mice were inoculated intraperitoneally with LP-BM5 and then injected every week with either an antibody against IP-10 or a control antibody. Eight weeks after infection, we analyzed the effect of IP-10 neutralization. Anti-IP-10 antibody treatment did not change the generalized lymphadenopathy and hepatosplenomegaly of mice with MAIDS. The treatment significantly reduced the number of IP-10- and CXCR3-positive cells in the mesenteric lymph nodes (mLNs) but not the phenotypes and gross numbers of cells. In contrast, IP-10 neutralization reduced the number of mononuclear cells infiltrating into the pancreas. Anti-IP-10 antibody treatment did not change the numbers of IFN-γ^+ and $IL10^+$ cells in the mLN but significantly reduced their numbers, especially IFN-γ^+ and IL-10^+ $CD4^+$ T cells and IFN-γ^+ Mac-1^+ cells, in the pancreas. IP-10 neutralization ameliorated the pancreatic lesions of mice with MAIDS probably by blocking the cellular infiltration of $CD4^+$ T cells and IFN-γ^+ Mac-1^+ cells into the pancreas at least at 8 wk after infection, suggesting that IP-10 and these cells might play a key role in the development of chronic autoimmune pancreatitis.

autoimmune pancreatitis; Sjögren's syndrome; murine acquired immodeficiency syndrome; chemokines; interferon-γ-inducible protein 10

CHEMOKINES, which are chemotactic cytokines, control the essential process of the attraction of leukocytes to the tissues in inflammation (1, 18). The chemokine family comprises two major subfamilies, termed CXC and CC according to the arrangement of the first two conserved cysteines, which are separated by one amino acid and are adjacent, respectively (1, 18). Interferon (IFN)-γ-inducible protein of 10 kDa (IP-10/CXCL10) is a member of the CXC chemokine family and a potent chemoattractant for activated T lymphocytes, natural killer cells, and monocytes (6, 17). It is also considered as a regulator of T helper (Th)1 inflammatory responses (26). The expression of IP-10 was elevated in several diseases such as ulcerative colitis (34), hepatitis (21), multiple sclerosis (31), and Sjögren's syndrome (SjS) (22), suggesting the involvement of IP-10 in the development of these diseases. It has been recently reported that IP-10 is expressed by β-cells of the islets of Langerhans, resulting in the preferential accumulation of $CXCR3^+$ T cells into the pancreas in a virus-induced Type I diabetic mouse model (7). Information about the role of chemokines in pancreatic diseases, however, is limited and needs further investigation (2, 28). In the pathogenesis of chronic pancreatitis, especially with autoimmune etiology, the role of chemokines such as IP-10 has not been investigated thoroughly.

The LP-BM5 murine leukemia virus (MuLV) is a retrovirus that is known to induce profound immunodeficiency with splenomegaly and generalized lymphadenopathy in susceptible strains of mice, such as C57BL/6 (B6) mice, and occasionally brings about lymphoid malignancy (10, 14, 19). In the early phase of infection, hypergammaglobulinemia and polyclonal B and T cell activation are induced and autoantibodies such as anti-nuclear and anti-double-stranded DNA antibodies are detected in mice infected with the virus (10, 14, 19). In the late phase of infection, virus-infected B6 mice show symptoms similar to those of human acquired immunodeficiency syndrome (AIDS); therefore, they have been studied as a murine model of AIDS, termed as murine AIDS (MAIDS) (10, 14, 19). We have reported previously that systemic exocrinopathy resembling SjS was induced in systemic exocrine glands such as salivary glands and lachrymal glands and in the pancreas of virus-infected mice; thus we proposed that mice with MAIDS could be an animal model for SjS as well as AIDS (32, 33). In mice with MAIDS, the pancreatic lesions are the exocrine system-oriented inflammation characterized by cellular infil-

Address for reprint requests and other correspondence: K. Suzuki, Dept. of Gastroenterology and Hepatology, Niigata Univ. Graduate School of Medical and Dental Sciences, 1-757 Asahimachi-dori, Niigata 951-8510, Japan (e-mail: kjsuzuki@med.niigata-u.ac.jp).

The costs of publication of this article were defrayed in part by the payment of page charges. The article must therefore be hereby marked "*advertisement*" in accordance with 18 U.S.C. Section 1734 solely to indicate this fact.

tration around the interlobular pancreatic ducts and acinar cell destruction (32, 33, 35), but with no damage of the endocrine system, that is, the islets of Langerhans (35). The pancreas-infiltrating cells comprise both Th1- and Th2-type $CD4^+$ T cells, although with a predominance of Th2 cells over Th1 cells (35). Thus the pancreatic lesions of the mice have some similarities to autoimmune-related chronic pancreatitis, especially the lesions associated with SjS.

To clarify the role of IP-10 in the development of chronic pancreatitis with autoimmune etiology, especially associated with SjS, we investigated the effect of CXCL10 neutralization on pancreatic lesions of mice with MAIDS. Our results suggest that anti-IP-10 monoclonal antibody ameliorated the pancreatic lesions of mice with MAIDS.

MATERIALS AND METHODS

Animals. Four-week-old female B6 mice were purchased from Charles River Japan (Kanagawa, Japan) and maintained at the Animal Center of the Niigata University School of Medicine under specific-pathogen-free conditions. All animal experiments were performed according to the "Guide for Animal Experiments" of Niigata University School of Medicine.

Induction of MAIDS. LP-BM5 MuLV was prepared from the supernatant of cloned G6 cells infected with the retrovirus as reported previously (35). Four-week-old B6 female mice were injected intraperitoneally with 0.3 ml of LP-BM5 MuLV virus stock solution. At 8 wk after virus inoculation, mice with MAIDS were killed by cervical dislocation under ether anesthesia, and their pancreases were removed for further analysis. For blocking experiments, PBS containing 100 μg/100 μl anti-CXCL10 monoclonal antibodies (36) or anti-human parathyroid-related peptide monoclonal antibodies, which was the IgG_1 subclass-matched control monoclonal antibody, or PBS alone were administered intraperitoneally at the time of virus inoculation and once a week thereafter.

Monoclonal antibodies. For immunofluorescence (IF) and flow cytometric analyses, the following monoclonal antibodies were used: anti-CD4 (clone GK1.5, IgG_{2b}), anti-CD8 (clone 53-6.7, IgG_{2a}), anti-B220 (clone RA3-6B2, IgG_{2a}), anti-Mac-1 (clone M-70.15, IgG_{2b}), anti-mouse INF-γ (clone XMG1.2), and anti-mouse IL-10 (clone JES5-16E3). For immunostaining of IP-10 or CXCR3, goat polyclonal antibodies to IP-10 or CXCR3 (Santa Cruz Biotechnology; Santa Cruz, CA) were used.

Detection of LP-BM5 MuLV by PCR. The PCR method used for the detection of the virus was as reported previously (33).

Quantitative RT-PCR to detect cytokine mRNA. Total RNA was extracted from the mesenteric lymph node (mLN) and pancreas specimens with TRIzol (GIBCO-BRL) according to the standard protocol and reverse transcribed. Thereafter, cDNA was amplified using the ABI 7700 sequence detector system (Applied Biosystems; Foster City, CA) with a set of primers and probes corresponding to IFN-γ, IL-10, IP-10, CXCR3, and GAPDH as previously described (36).

Histopathological examination. Tissue samples were taken from the pancreas, fixed in 10% buffered formalin, and then embedded in paraffin wax blocks. Sections (4-μm thick) were made in the usual way and stained with hematoxylin and eosin. The stained sections were then examined by light microscopy.

The numbers of inflammatory cells in a high-power field (×400) were counted under a microscope, and the degree of pancreatitis was assessed from *0* to *4* as reported previously (11, 24).

IF staining procedure. Frozen sections of the pancreas were prepared in a cryostat and stained with several fluorescent dye-conjugated anti-mouse antibodies as described above. The sections were observed by fluorescence microscopy.

Double-IF staining procedure. For the simultaneous demonstration of cell surface antigens and cytokines, the IF staining method was as reported previously (35).

Statistical analysis. Data are expressed as means ± SD. Statistical analyses were performed using the unpaired Student's *t*-test or the nonparametric Mann-Whitney test. Differences were considered significant at $P < 0.05$.

RESULTS

IP-10 neutralization did not prevent infection by the MAIDS virus. All mice infected with LP-BM5 MuLV developed characteristic MAIDS symptoms such as generalized lymphadenopathy and hepatosplenomegaly ($n = 15$), and neutralization of IP-10 did not change the course of MAIDS ($n = 15$). Eight weeks after the virus inoculation, there were no differences in the weights of the liver, spleen, and mLNs between mice with MAIDS injected with anti-IP-10 monoclonal antibody and those injected with control antibody (Fig. 1*A*). A defective LP-BM5 virus genome was detected in mice of both groups by

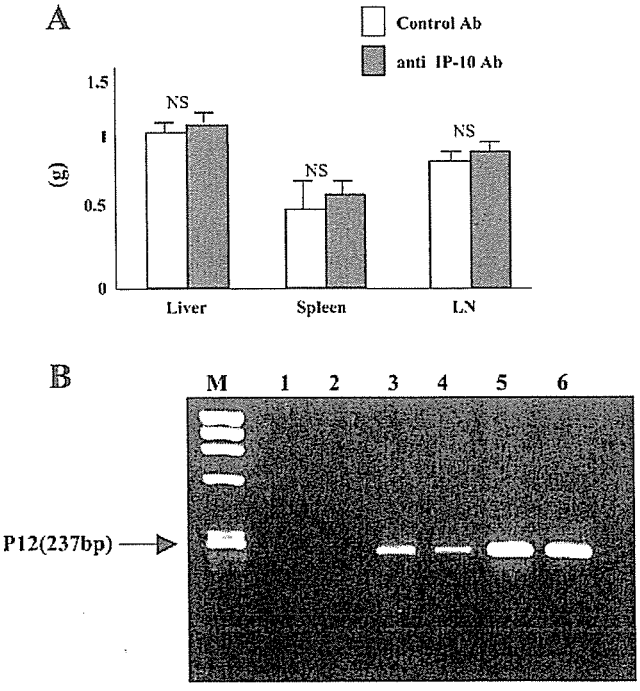

Fig. 1. Effect of neutralization of interferon (IFN)-γ-inducible protein of 10 kDa (IP-10/CXCL10) on the course of murine acquired immunodeficiency syndrome (MAIDS). *A*: effect of neutralization of IP-10 on organs of mice with MAIDS. The weights of the liver, spleen, and mesenteric lymph nodes (LNs) of mice with MAIDS injected with control antibody (Ab) were increased at 8 wk after infection. However, they were not changed after the injection of anti-IP-10 monoclonal (m)Ab. Data are means ± SD. NS, not significant. *B*: neutralization of IP-10 did not prevent infection by the MAIDS virus. LP-BM5 murine leukemia virus (MuLV) was detected in the mesenteric LNs and pancreas of mice with MAIDS at 8 wk after infection. Template DNAs were extracted from frozen sections of the pancreas and then analyzed by PCR with P12 primer. The bands were obtained by running the PCR products in agarose gel. M, molecular size marker; *lane 1*, the mesenteric LN of an uninfected C57BL/6 (B6) mouse (negative control); *lane 2*, the pancreas of an uninfected B6 mice (negative control); *lane 3*, the mesenteric LN of a mouse with MAIDS injected with control Ab; *lane 4*, the pancreas of a mouse with MAIDS injected with control Ab; *lane 5*, the mesenteric LN of a mouse with MAIDS injected with anti-IP-10 mAb; *lane 6*, the pancreas of a mouse with MAIDS injected with anti-IP-10 mAb.

PCR in the same frozen sections of the mLNs and pancreas of mice with MAIDS as those used for immunohistochemical staining (Fig. 1*B*). P12 of the virus genome was not detected in untreated normal B6 mice (Fig. 1*B*).

Effect of IP-10 neutralization on the expression of IP-10 and CXCR3 by lymphoid cells in mice with MAIDS. In the mLN and pancreas of mice with MAIDS injected with control antibody, the expression levels of mRNA for IP-10 and its receptor CXCR3 were significantly increased compared with untreated B6 mice (Fig. 2*A*). Neutralization of IP-10 down-regulated the expression of mRNA for IP-10 and CXCR3 in the mLNs and pancreas of mice with MAIDS (Fig. 2, *A* and *B*). Next, we analyzed their expressions in the pancreas and mLN by IF. In normal mice, IP-10 and CXCR3 were detected neither in the mLN nor in the pancreas, with the exception of a few $CXCR3^+$ cells scattered in the mLN (data not shown). The numbers of cells that expressed IP-10 and CXCR3 increased in the mLN and pancreas of mice with MAIDS injected with control antibody (Fig. 3*I*, *A* and *B*, and *II*, *A* and *B*). Double-color IF revealed that in the mLN, some $IP\text{-}10^+$ cells were $Mac\text{-}1^+$ cells and $CXCR3^+$ cells were mainly $CD4^+$ T cells (Fig. 3*I*, *C* and *D*). In the pancreas of mice with MAIDS, IP-10 and CXCR3 were mainly detected on some cells in an inflammatory cell focus around the pancreatic duct (Fig. 3*II*, *A* and *B*). Double-color IF showed that $IP\text{-}10^+$ cells were not positive for CD4, CD8, B220, and Mac-1 (Fig. 3*II*, *C*). It also revealed that $CXCR3^+$ cells were mainly $CD4^+$ T cells (Fig. 3*II*, *D*). Interestingly, IP-10 was also detected on some cells localized between the basal laminas that envelope each acinus of a minimal functional unit of the exocrine system of the pancreas (Fig. 3*II*, *A*, *inset*). Neutralization of IP-10 decreased the numbers of cells that expressed IP-10 or CXCR3 in the mLN (Fig. 3*I*, *E* and *F*) and pancreas (Fig. 3*II*, *E* and *F*) of mice with MAIDS.

Effect of IP-10 neutralization on mLN cells of mice with MAIDS. IF study of the mLN revealed that the numbers of $CD4^+$, $CD8^+$, $B220^+$, and $Mac\text{-}1^+$ cells were unchanged statistically by neutralization of IP-10 (Fig. 4*A*).

To reveal the systemic effect of IP-10 neutralization on cytokine production, we analyzed the number of IFN-γ- and IL-10-positive cells in the mLN of mice with MAIDS at 8 wk after infection by IF. We chose IFN-γ as a representative for a proinflammatory cytokine (or Th1 response) and IL-10 as a representative of an anti-inflammatory cytokine (or Th2). In mLNs of mice with MAIDS, there was no significant difference between the anti-IP-10 monoclonal antibody-treated group and the control antibody-treated group in IL-10- and IFN-γ-positive cells (Fig. 4*B*). IP-10 neutralization did not change the number of these cytokine-positive cells in the mLN of mice with MAIDS (Fig. 4*B*).

IP-10 neutralization ameliorated pancreatic lesions of mice with MAIDS. We have previously reported that periductal mononuclear cellular infiltration resembling autoimmune pancreatitis associated with SjS was detected in mice with MAIDS

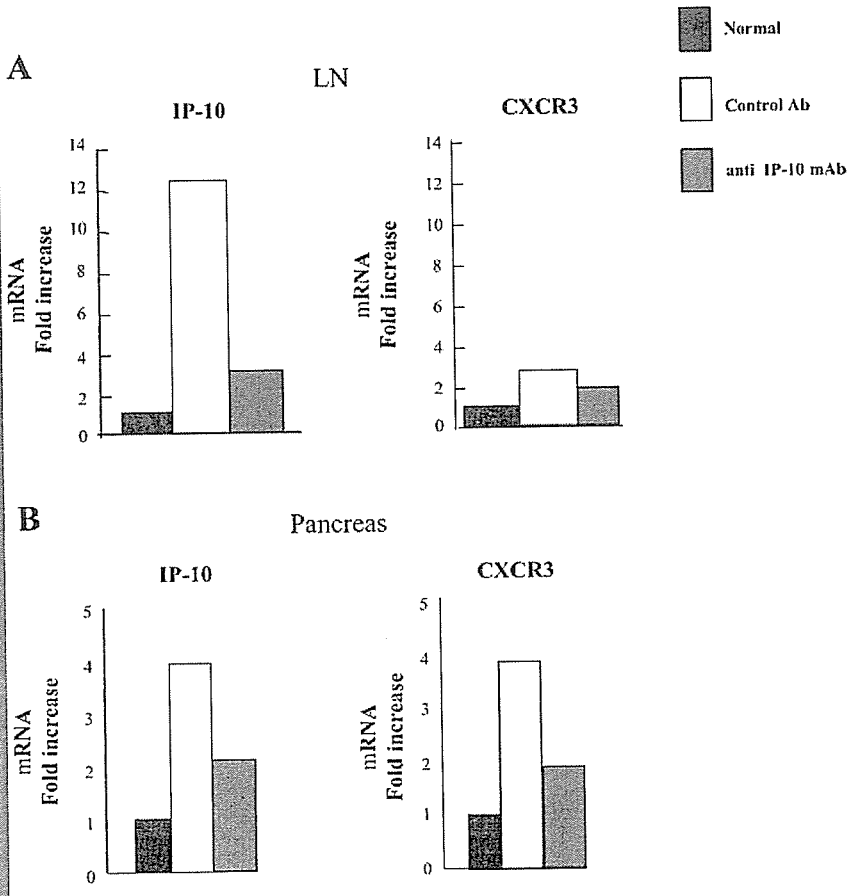

Fig. 2. Real-time quantitative PCR analysis of IP-10 and CXCR3 mRNA expression. The expressions of IP-10 and CXCR3 mRNA of the mesenteric LNs (*A*) and pancreas (*B*) were analyzed. Each amount was normalized to the level of each GAPDH. Final relative values are expressed relative to the calibrators (Ref. 36) as described above.

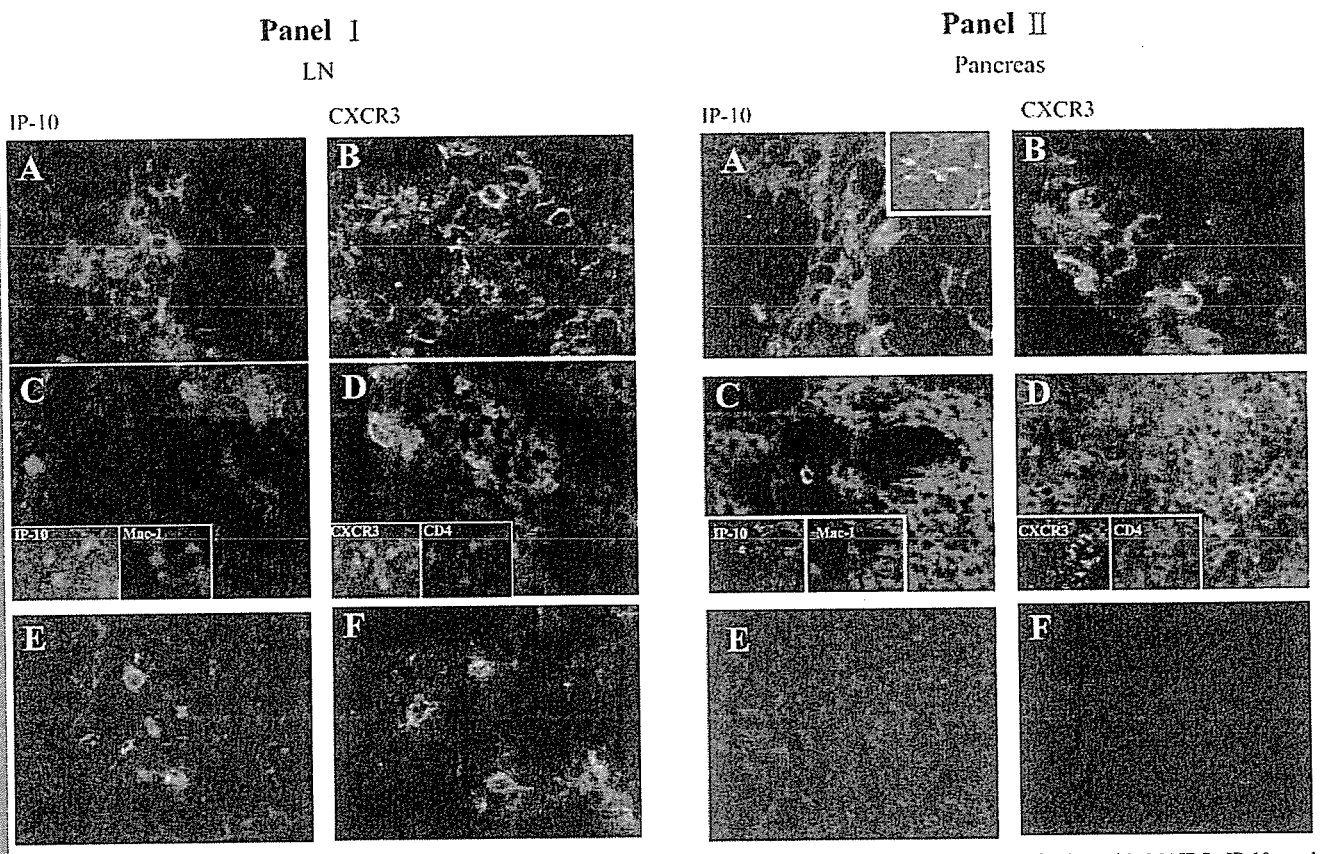

Fig. 3. *I*: effect of neutralization of IP-10/CXCL10 on the expressions of IP-10 and CXCR3 in the mesenteric LNs of mice with MAIDS. IP-10- and CXCR3-positive cells were detected in the mesenteric LNs of mice with MAIDS injected with control Ab (*A* and *B*). Their numbers decreased in the mesenteric LNs of mice with MAIDS injected with anti-IP-10 mAb (*E* and *F*). Some of the IP-10$^+$ cells (green) were Mac-1$^+$ cells (red), but were never positive for CD4, CD8, or B220 (*C*). Most of the CXCR3$^+$ cells (green) were positive for CD4 (red) (*D*). IP-10 was not detected, but CXCR3 was detected on a few cells in the mesenteric LN of an untreated B6 mouse (data not shown). *A*, *C*, and *E*, anti-IP-10 mAb-stained sections; *B*, *D*, and *F*, other sections stained with anti-CXCR3 Ab. *II*: effect of neutralization of IP-10 on the expressions of IP-10 and CXCR3 in the pancreas of mice with MAIDS. IP-10-and CXCR3-positive cells were detected in the pancreas of mice with MAIDS injected with control Ab (*A* and *B*). In the pancreas of mice with MAIDS, IP-10 and CXCR3 were mainly detected on some cells in a inflammatory cell focus around a pancreatic duct (*A* and *B*). Interestingly, IP-10 was also detected on cells localized between basal laminas that envelope each acinus of a minimal functional unit of the exocrine system of the pancreas (*A*, *inset*). IP-10$^+$ cells (green) were not positive for Mac-1$^+$ cells (red), CD4, CD8, or B220 (*C*). Most of the CXCR3$^+$ cells (green) were positive for CD4 (red) (*D*). IP-10 was not detected, but CXCR3 was detected on a few cells in the mesenteric LN of an untreated B6 mouse (data not shown). IP-10-and CXCR3-positive cells were not detected in the pancreas of mice with MAIDS injected with anti-IP-10 mAb (*E* and *F*). IP-10 and CXCR3 were not detected in the pancreas of an untreated B6 mouse (*A* and *B*). *A*, *C*, and *E*, sections stained with anti-IP-10 mAb; *B*, *D*, and *F*, sections stained with anti-CXCR3 Ab.

and the numbers of infiltrating cells and the grades of the lesions reached a peak at 8 wk after infection. To evaluate the effect of IP-10 neutralization, we, therefore, analyzed the pancreatic lesions of mice with MAIDS at 8 wk after infection. In mice with MAIDS injected with control antibody, inflammatory cells were detected around the pancreatic ducts, from where they progressively expanded, pressing the acinar architecture outward (Fig. 5*A*). At the interface lesions between the infiltrating cells and pancreatic parenchyma, destructed acinar cells were detected, but the degree of acinar cell destruction by infiltrating cells was rather mild (Fig. 5*C*). Peri-islet cellular infiltration was also observed (Fig. 5, *A* and *C*). Anti-IP-10 monoclonal antibody treatment clearly ameliorated the pathological lesions of the pancreas of mice with MAIDS (Fig. 5, *B* and *D*); the size of periductal cellular infiltration became smaller and the numbers of destructed acinar cells were also decreased (Fig. 5, *B* and *D*). Both the numbers of pancreas-infiltrating cells and the histological grading scores of the pancreatitis were significantly reduced by IP-10 neutralization (Fig. 5, *E* and *F*).

IP-10 neutralization ameliorated pancreatic lesions through decreased migration of CD4$^+$T, Mac-1$^+$, and B220$^+$ cells in mice with MAIDS. Eight weeks after infection, pancreas-infiltrating cells were composed of CD4$^+$ and CD8$^+$ T cells, Mac-1$^+$ macrophages, and B220$^+$ B cells but not natural killer cells or granulocytes. The major populations of infiltrating cells were composed CD4$^+$ T cells, Mac-1$^+$ macrophages, and B220$^+$ cells (Fig. 6, *A*, *C*, *E*, and *G*). The IF study showed that IP-10 neutralization significantly decreased the numbers of CD4$^+$ T, Mac-1$^+$, and B220$^+$ cells in pancreatic lesions of mice with MAIDS (Fig. 6, *B*, *D*, *F*, and *G*).

IP-10 neutralization decreased the migration of IFN-γ- and IL-10-producing CD4$^+$T and Mac-1$^+$ cells in the pancreas of mice with MAIDS. To reveal the effect of IP-10 neutralization on the immune response in the pancreas of mice with MAIDS, we analyzed the cytokine expression of IFN-γ and IL-10. The

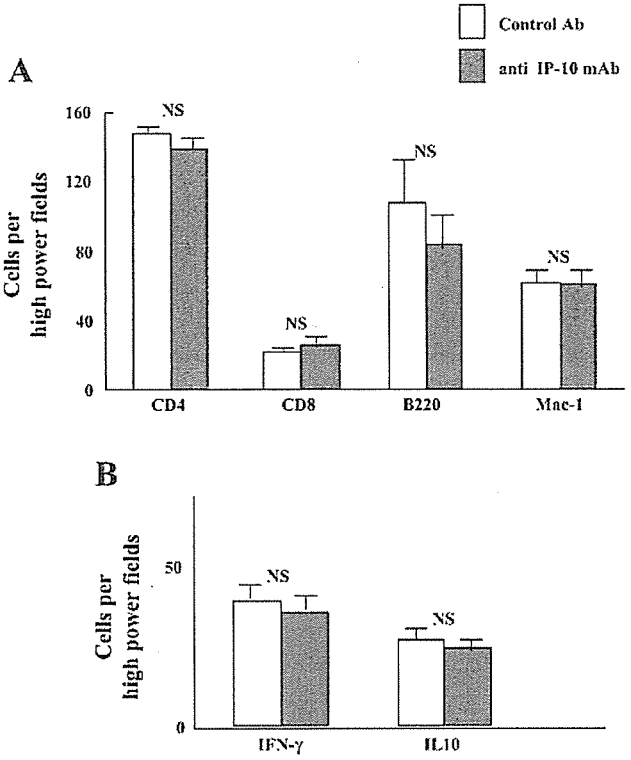

Fig. 4. Effect of neutralization of IP-10/CXCL10 on lymphocyte subpopulations in the LNs of mice with MAIDS. *A*: quantitative analysis of immune cells in the LNs by immunofluorescence (IF) for CD4, CD8, Mac-1, and B220. *B*: quantitative analysis of IFN-γ and IL-10 expression in the mesenteric LNs of mice with MAIDS at 8 wk after infection. Each focus of cellular infiltration was examined for the presence of CD4, CD8, B220, Mac-1, IFN-γ, and IL-10 cells. Final results are presented as the numbers of cells per high-powered microscope field. Representative findings (means ± SD; n = 10) from 3 independent experiments are shown.

levels of expression of the mRNAs of both cytokines in the pancreas were significantly increased after infection, and IP-10 neutralization decreased them (Fig. 7*A*). IF showed that IP-10 neutralization significantly decreased the numbers of IFN-γ- and IL-10-positive cells in the pancreas of mice with MAIDS (Fig. 7*B*).

Next, by the double-color IF method, we characterized the phenotypes of cells producing these cytokines. IFN-γ and IL-10 were mainly present on $CD4^+$ T cells (Fig. 8, *A* and *C*) and Mac-1^+ cells (Fig. 8, *E* and *G*) but not on $B220^+$ cells or $CD8^+$ T cells (data not shown). We did not detect the expression of IFN-γ or IL-10 in the pancreas of normal B6 mice (data not shown).

The numbers of IFN-γ- and IL-10-positive $CD4^+$ T cells were significantly reduced in mice with MAIDS by IP-10 neutralization (Figs. 7*C* and 8, *B* and D). Additionally, IP-10 neutralization significantly reduced the numbers of IFN-γ-positive Mac-1^+ cells in the pancreas of mice with MAIDS (Figs. 7*D* and 8*F*). The numbers of IL-10-positive Mac-1^+ cells became smaller by IP-10 neutralization, but there was no statistical significance between the mice with or without treatment (Figs. 7*D* and 8, *G* and *H*).

DISCUSSION

We have shown that systemic exocrinopathy including exocrine pancreatitis-like injury developed concordantly with the progression of MAIDS symptoms. Therefore, exocrine pancreatitis-like injury of mice with MAIDS might be a manifestation of several characteristic symptoms of MAIDS such as hepatomegaly, splenomegaly, systemic lymphadenopathy, and abnormal immunological reactions. In this study, we have shown that IP-10 neutralization ameliorated the pancreatic lesions of mice with MAIDS (Fig. 5) but prevented neither the infection nor the course of MAIDS (Fig. 1). These results suggest a different mechanism for the pathogenesis of systemic exocrinopathy including exocrine pancreatitis-like injury of MAIDS and the other MAIDS symptoms.

In the *Toxoplasma gondii* infection model, IP-10 neutralization inhibited the accumulation of effector T cells, resulting in a decreased ability to kill the parasite in target organs such as the liver, spleen, brain, and lung (12). IP-10 neutralization studies and a study on IP-$10^{-/-}$ mice also showed that the blockade of effector cell trafficking resulted in the breakdown of host defenses in neurotropic mouse hepatitis virus infection in the brain (5, 16). In the liver of patients with chronic active hepatitis C, we (21) have reported that IP-10 mRNA was expressed mainly in hepatocytes around intralobular focal and periportal piecemeal necrosis. These examples suggest that if the organ of the specific lesions induced by a particular infection was the same as the target organ of the infectious agent, IP-10 neutralization could ameliorate the organ lesions by inhibiting the trafficking of effector cells that eliminate the infectious agents from the target organ. In MAIDS, we reported previously that the virus was integrated in Ly-1 B cells but not in T cells (9) or on parenchymal cells of the pancreas (unpublished observations), although several reports have shown that B cells (13) and macrophages (4) as well as T cells (15) can serve as targets for infection of the virus. Therefore, pancreatic tissues are not the direct target cells of LP-BM5 infection, and the IP-10 neutralization-induced amelioration of pancreatic lesions of MAIDS cannot be explained by the decreased accumulation of effector cells that eliminate LP-BM5 from the pancreas.

We and others have reported that systemic exocrinopathy including pancreatitis-like injury is the characteristic organ lesions of mice with MAIDS (10, 14, 19, 32, 33, 35); however, the target antigen in exocrine glands, which regulates the target organ specificity, has been unknown. Without knowing the target antigen, delineating the process of inflammatory cell infiltration provides a basis for understanding the development of the pancreatic lesions of MAIDS. The blocking activity of the anti-IP-10 monoclonal antibody used in this study was confirmed in the chemotactic assay and in some other murine models depicting acute colitis (27) and encephalomyelitis (20). We confirmed that the anti-IP-10 monoclonal antibody had no cross-reactivity with other chemokines such as the monokine induced by IFN-γ, macrophage inflammatory protein-1α, or mature dendritic cells (36). In this study, therefore, we examined the expression of IP-10 and its receptor CXCR3 in the mLN and pancreas of mice with MAIDS. In the mLN and pancreas of MAIDS, IP-10 was mainly expressed on Mac-1^+ cells and CXCR3 was mainly detected on $CD4^+$ T cells. Anti-IP-10 treatment clearly reduced the number of these cells in both the mLN and pancreas. Our results suggest that cell trafficking into the pancreas of mice with MAIDS is carried out by the interaction between IP-10 and CXCR3 of $CD4^+$ cells. In the virus-induced Type I diabetes mouse model, it has been

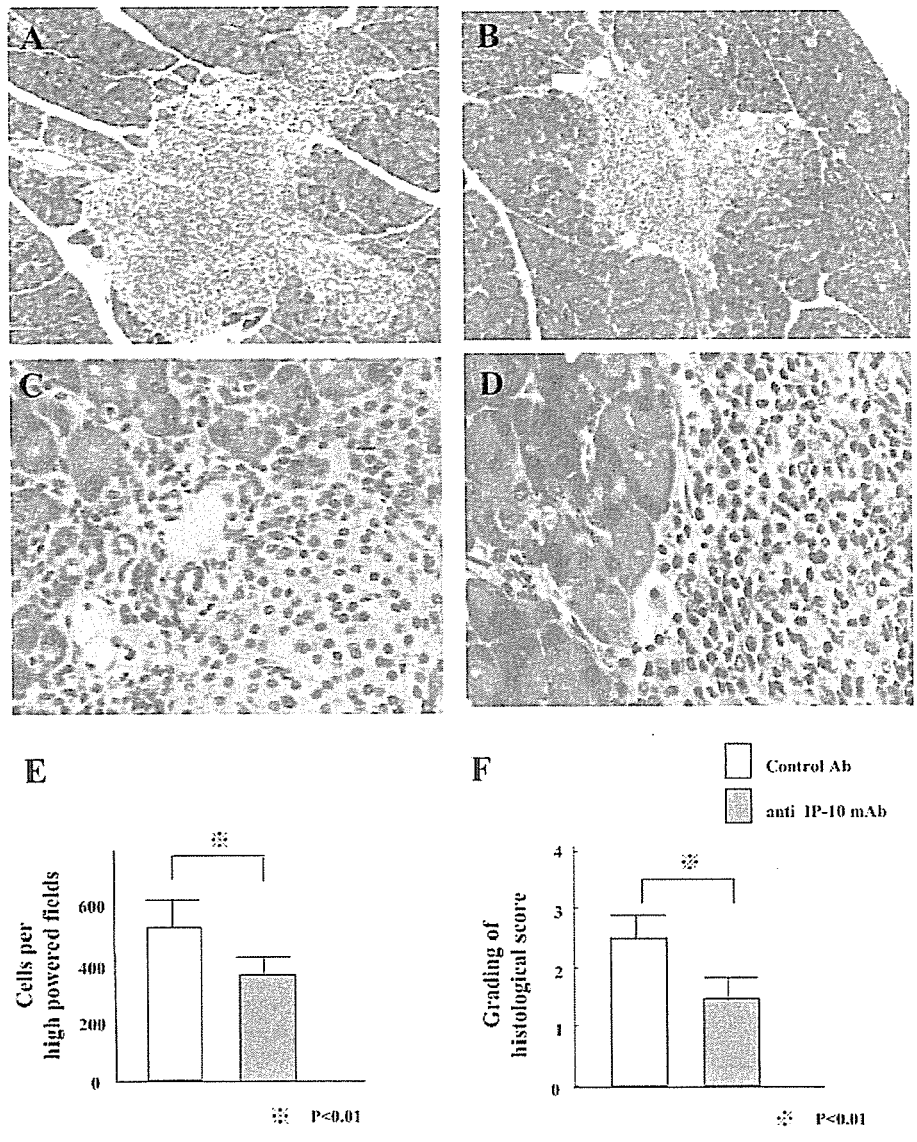

Fig. 5. Amelioration of pancreatic lesions of mice with MAIDS by neutralization of IP-10/CXCL10. *A* and *C*: pancreas from mice infected with LP-BM5 MuLV treated with control Ab at 8 wk after infection; *B* and *D*: pancreas from mice infected with LP-BM5 MuLV treated with anti-IP-10 mAb at 8 wk after infection. Sections were stained with hematoxylin and eosin. Original magnification: ×200 in *A* and *B* and ×400 in *C* and *D*. *E*: numbers of cells infiltrating the pancreas after infection. *F*: histological scores of acinar cell destruction of the pancreas at 8 wk after infection. Cells were counted under a microscope at high-power magnification for 3 different areas/mouse, and data of each time point were collected from 3 mice and compared with each other. *Data are significantly different between mice injected with anti-IP-10 mAb and those injected with control Ab as determined by Student's *t*-test ($P < 0.01$).

shown that β-cells of the islets of Langerhans produce chemokines including IP-10 with preferential attraction to T cells via CXCR3 (7). In our colitis model and those of others, IP-10 expression was confirmed in the colon epithelial cells, and IP-10 neutralization was shown to ameliorate the colitis with decreased $CXCR3^+$ cells in the colon (27, 29). In addition, Sugai et al. (22) reported that IP-10 is expressed on duct epithelial cells in salivary glands of patients with SjS. Contrary to these reports, we could not detect IP-10 expression on acinar cells or duct epithelial cells but found that IP-10 and CXCR3 were mainly expressed on cells in inflammatory foci around pancreatic ducts. Thus the lack of expression of IP-10 on target acinar cells and duct epithelial cells might be attributed to the mild pancreatitis-like injury of mice with MAIDS. Interestingly, IP-10 was also detected on cells localized between the basal laminas that envelope each acinus of a minimal functional unit of the exocrine system of the pancreas (Fig. 3*II*, *A*, *inset*). These cells disappeared together with the decreased numbers of pancreas-infiltrating cells after the neutralization of IP-10 (Fig. 3*II*, *A* and *C*). Therefore, we need to identify the nature of the $IP\text{-}10^+$ cells localized between basal laminas around each acinus, which are supposed to play a pivotal role in the recruitment of $CXCR3^+$ inflammatory cells into the pancreas of mice with MAIDS.

Recently, a Th1 and Th2 imbalance has been considered as one of the important mechanisms in the development of some autoimmune diseases (25). In our previous studies on the experimental models of encephalomyelitis (20), hepatitis (36), and Thy1.1 glomerulonephritis (8), we reported that anti-IP-10 monoclonal antibody treatment did not affect the cytokine environment of Th1/Th2 polarization. Considering these previous reports together with the observations of this study, it is conceivable that the IP-10 neutralization-induced amelioration of the pancreatic lesions of MAIDS did not result from the rectification of the cytokine environment of Th1/Th2 imbalance but rather from blockade of trafficking of inflammatory cells into the pancreas.

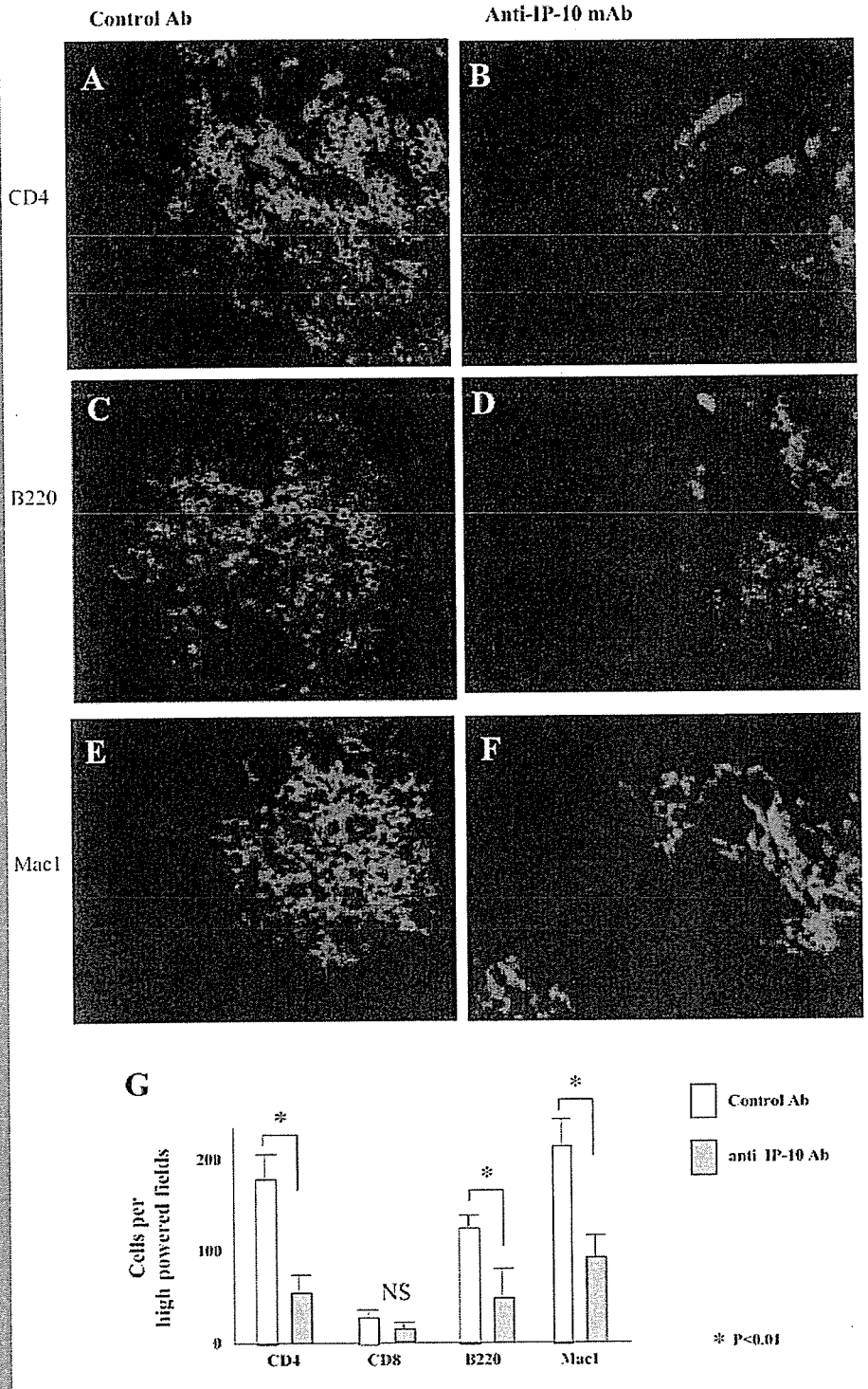

Fig. 6. Effect of neutralization of IP-10/CXCL10 on lymphocyte subpopulations in the pancreas of mice with MAIDS. IF analysis revealed the decreased numbers of CD4 (*A* and *B*), CD8 (data not shown), B220 (*C* and *D*), and Mac-1 (*E* and *F*) immune cells in the pancreas after blockade of IP-10. *G*: quantitative analysis of CD4, CD8, Mac-1, and B220 expression in the pancreas of mice with MAIDS at 8 wk after infection. Each focus of cellular infiltration was examined for the presence of CD4, CD8, B220, and Mac-1 cells. Final results are presented as the numbers of cells per high-powered microscope field. Representative findings (means ± SD; $n = 10$) from 3 independent experiments are shown. *Data are significantly different between mice injected with anti-IP-10 mAb and those injected with control Ab as determined by Student's *t*-test ($P < 0.01$).

In MAIDS, pancreas-infiltrating cells are mainly composed of $CD4^+$T cells, $B220^+$B cells, and Mac-1^+ macrophages (Fig. 6). Neutralization of IP-10 clearly and selectively decreased the numbers of these cells in the pancreas but not in the mLN of mice with MAIDS (Figs. 3–8). Flow cytometric analyses revealed the reciprocal quantitative change of cell phenotype between the mLN and pancreas. That is, IP-10 neutralization increased the numbers of $CD3^+$, $CD4^+$, and αβT cells as well as Mac-1^+ cells in the mLN but decreased the numbers of those cells in the pancreas of mice with MAIDS (unpublished observations). These results suggest that IP-10 plays a pivotal role in the migration of inflammatory cells between the pancreas and mLN. IP-10-CXCR3 interactions, with Th1-dependent immunity, have been observed in several

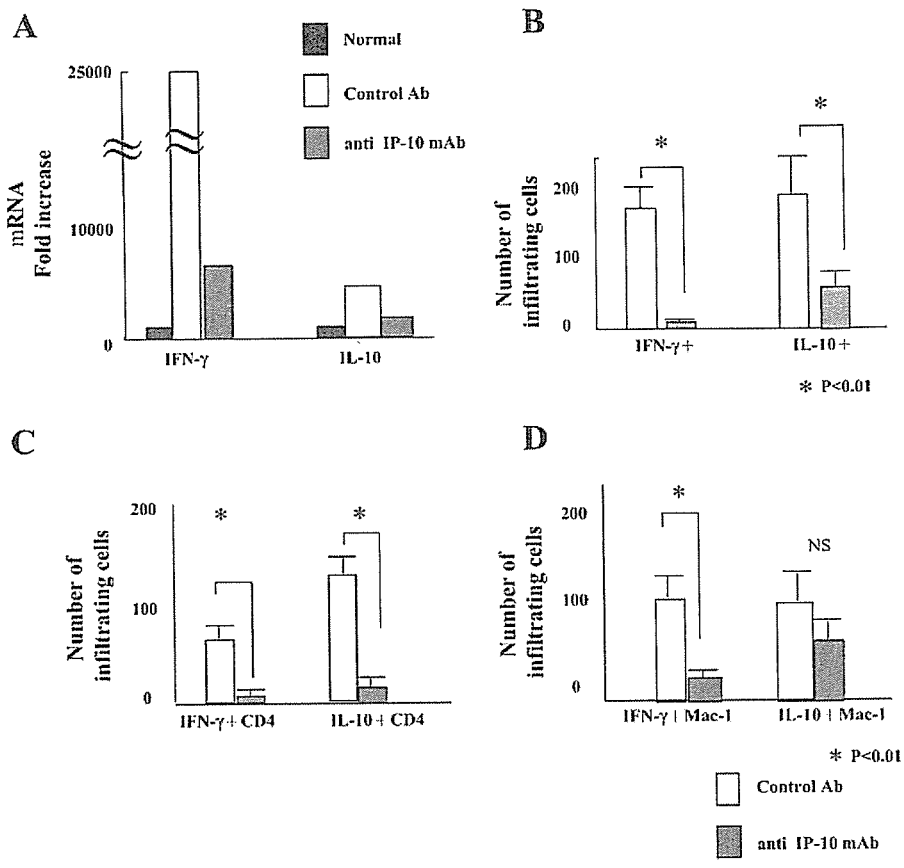

Fig. 7. Effects of blockade of IP-10/CXCL10 on cytokine production by inflammatory cells infiltrating the pancreas in mice with MAIDS. *A*: real-time quantitative PCR of IFN-γ and IL-10 mRNA expression in the pancreas of mice with MAIDS. Each amount was normalized to the level of GAPDH, and the final relative values are expressed relative to calibrators on *day 0*. *B*: numbers of pancreas-infiltrating cells that expressed IFN-γ and IL-10 at 8 wk after infection. Stained cryostat sections of 3 focuses of cellular infiltration of the individual pancreas were examined by counting the numbers of cells expressing IFN-γ and cells expressing IL-10. Three mice were analyzed for each time point. In control normal B6 mice, a negligible number of cells expressed IFN-γ or IL-10, so data are not shown. *C* and *D*: quantitative analysis of IFN-γ and IL-10 expression patterns of $CD4^+$ and Mac-1^+ cells that infiltrated the pancreas at 8 wk after infection. Stained cryostat sections of 3 focuses of cellular infiltration of the individual pancreas were examined by counting the numbers of $CD4^+$ cells expressing IFN-γ or IL-10 (*C*) and Mac-1^+ cells expressing IFN-γ or IL-10 (*D*). Three mice were analyzed for each time point. In control normal B6 mice, a negligible number of cells expressed IFN-γ or IL-10, so data are not shown. *Data are significantly different between mice injected with anti-IP-10 mAb and those injected with control Ab as determined by Student's *t*-test ($P < 0.01$).

inflammatory diseases, including multiple sclerosis (23, 30) and inflammatory bowel diseases (34). In animal models of these diseases, IP-10 neutralization or gene disruption of IP-10 clearly showed that amelioration of the diseases was achieved mainly by blocking $CXCR3^+$ cell trafficking into the IP-10-expressing target organs (5, 27, 29, 36). The ligands CXCL9, CXCL10, and CXCL11 bind to the CXCR3 receptor and share the ability to activate biochemical and functional events in target cells. All these ligands recruit $CXCR3^+$ cells; hence, neutralization of any of these ligands may not be sufficient to significantly abrogate the underlying biology of $CXCR3^+$ cells, but the use of CXCR3-deficient mice and IFN-γ neutralization will elucidate the role of these cells and cytokines in our model in future study. In this study, neutralization of IP-10 decreased not only the numbers of IFN-γ^+ $CD4^+$ T cells but also IL-10^+ $CD4^+$ T and IFN-γ^+ Mac-1^+ cells (Figs. 7 and 8). In an autoimmune diabetic mouse model injected with islet-specific Th1 $CD4^+$ T cells, insulitis was induced by the first accumulation of $CD4^+$ T cells followed by infiltration of Mac-1^+ cells (3). The inflammatory cells that infiltrated initially to the pancreas, therefore, might be the organ-specific autoreactive $CXCR3^+$ IFN-γ^+ $CD4^+$ T cells, and they then produce other cytokines and chemokines to attract the other IL-10^+ $CD4^+$ T cells and IFN-γ^+ Mac-1^+ cells into the pancreas of mice with MAIDS. In this study, we analyzed the effect of IP-10 neutralization only at one time point; however, the effects of the treatment on virus-induced inflammatory infiltrate and cytokine expression are most likely time dependent. Thus we need to analyze the kinetics of the responses in future study. IL-10^+ Mac-1^+ cells in the pancreatic lesions of mice with MAIDS were not significantly reduced by neutralization of IP-10 (Fig. 8), and the function of these cells in the formation of the lesions should be elucidated in future study. In conclusion, IP-10 neutralization could be a unique organ-specific therapeutic strategy for chronic pancreatitis, especially autoimmune pancreatitis associated with SjS.

ACKNOWLEDGMENTS

We thank Dr. Xiu-Hua Yang and Norio Honda for technical assistance and Dr. Minoru Nomoto and Dr. Terasu Honma for helpful discussions.

GRANTS

This work was supported by grants from the Ministry of Education and Science and Technology and the Ministry of Health, Welfare, and Labor of the Government of Japan.

REFERENCES

1. **Baggiolini M.** Chemokines and leukocyte traffic. *Nature* 392: 565–568, 1998.
2. **Bhatia M, Brady M, Shokuhi S, Christmas S, Neoptolemos JP, and Slavin J.** Inflammatory mediators in acute pancreatitis. *J Pathol* 190: 117–125, 2000.
3. **Bradley LM, Asensio VC, Schioetz LK, Harbertson J, Krahl T, Patstone G, Woolf N, Campbell IL, and Sarvetnick N.** Islet-specific Th1, but not Th2, cells secrete multiple chemokines and promote rapid induction of autoimmune diabetes. *J Immunol* 162: 2511–2520, 1999.
4. **Cheung SC, Chattopadhyay SK, Hartley JW, Morse 3rd HC, and Pitha PM.** Aberrant expression of cytokine genes in peritoneal macro-

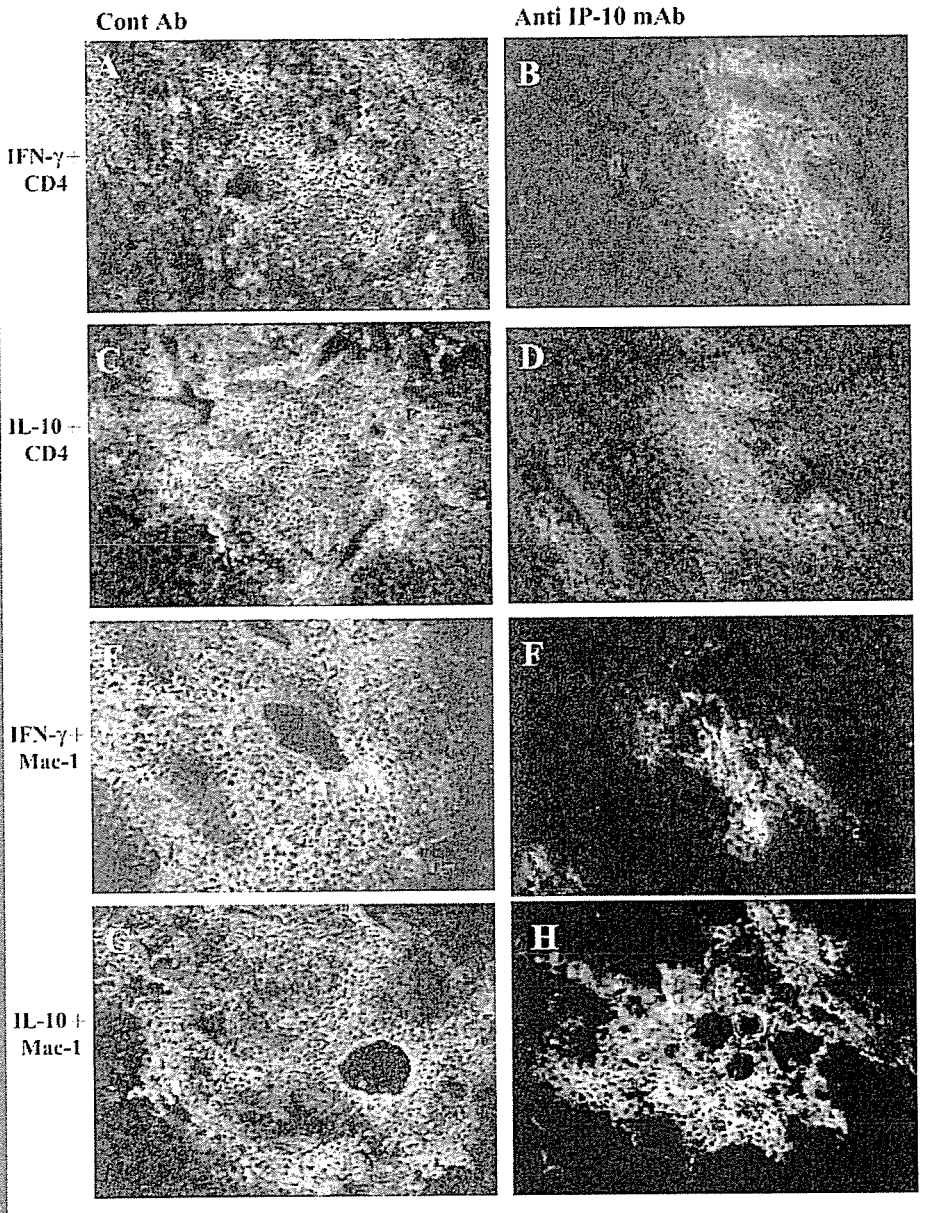

Fig. 8. Effects of blockade of IP-10/CXCL10 by a dual-labeling IF study of cytokine expression with cellular markers in the pancreas of mice with MAIDS. The numbers of cytokine-expressing cells were reduced by neutralization of CXCL10. Shown are sections of the pancreas of mice injected with control Ab (*A*, *C*, *E*, and *G*) or anti-IP-10 mAb (*B*, *D*, *F*, and *H*) at 8 wk after infection. *A–H*: double-color IF staining for CD4 and IFN-γ (*A* and *B*), CD4 and IL-10 (*C* and *D*), Mac-1 and IFN-γ (*E* and *F*), and Mac-1 and IL-10 (*G* and *H*) of the pancreas of mice with MAIDS at 8 wk after infection. *A–D*: CD4 (red); *E–H*: Mac-1 (red); *A*, *B*, *E*, and *F*: IFN-γ (green); *C*, *D*, *G*, and *H*: IL-10 (green).

phages from mice infected with LP-BM5 MuLV, a murine model of AIDS. *J Immunol* 146: 121–127, 1991.

5. **Dufour JH, Dziejman M, Liu MT, Leung JH, Lane TE, and Luster AD.** IFN-γ-inducible protein 10 (IP-10; CXCL10)-deficient mice reveal a role for IP-10 in effector T cell generation and trafficking. *J Immunol* 168: 3195–3204, 2002.
6. **Farber JM.** Mig and IP-10: CXC chemokines that target lymphocytes. *J Leukoc Biol* 61: 246–257, 1997.
7. **Frigerio S, Junt T, Lu B, Gerard C, Zumsteg U, Hollander GA, and Piali L.** β-Cells are responsible for CXCR3-mediated T-cell infiltration in insulitis. *Nat Med* 8: 1414–1420, 2002.
8. **Han GD, Koike H, Nakatsue T, Suzuki K, Yoneyama H, Narumi S, Kobayashi N, Mundel P, Shimizu F, and Kawachi H.** IFN-inducible protein-10 has a differential role in podocyte during Thy1.1 glomerulonephritis. *J Am Soc Nephrol* 14: 3111–3126, 2003.
9. **Hitoshi Y, Okada Y, Sonoda E, Tominaga A, Makino M, Suzuki K, Kinoshita J, Komuro K, Mizuochi T, and Takatsu K.** Delayed progression of a murine retrovirus-induced acquired immunodeficiency syndrome in X-linked immunodeficient mice. *J Exp Med* 177: 621–626, 1993.
10. **Jolicoeur P.** Murine acquired immunodeficiency syndrome (MAIDS): an animal model to study the AIDS pathogenesis. *FASEB J* 5: 2398–2405, 1991.
11. **Kannno H, Nose M, Itoh J, Taniguchi Y, and Kyogoku M.** Spontaneous development of pancreatitis in the MRL/Mp strain of mice in autoimmune mechanism. *Clin Exp Immunol* 89: 68–73, 1992.
12. **Khan IA, MacLean JA, Lee FS, Casciotti L, DeHaan E, Schwartzman JD, and Luster AD.** IP-10 is critical for effector T cell trafficking and host survival in *Toxoplasma gondii* infection. *Immunity* 12: 483–494, 2000.
13. **Kim WK, Tang Y, Kenny JJ, Longo DL, and Morse HC 3rd.** In murine AIDS, B cells are early targets of defective virus and are required for efficient infection and expression of defective virus in T cells and macrophages. *J Virol* 68: 6767–6769, 1994.
14. **Klinken SP, Fredrickson TN, and Hartley JW.** Evolution of B cell lineage lymphomas in mice with a retrovirus-induced immunodeficiency syndrome, MAIDS. *J Immunol* 140: 1123–1131, 1998.
15. **Kubo Y, Nakagawa Y, Kakimi K, Matsui H, Iwashiro M, Kuribayashi K, Masuda T, Hiai H, Hirama T, Yanagawa S, and Ishimoto A.**

Presence of transplantable T-lymphoid cells in C57BL/6 mice infected with murine AIDS virus. *J Virol* 66: 5691–5695, 1992.
16. **Liu MT, Chen BP, Oertel P, Buchmeier MJ, Armstrong D, Hamilton TA, and Lane TE.** The T cell chemoattractant IFN-inducible protein 10 is essential in host defense against viral-induced neurologic disease. *J Immunol* 165: 2327- 2330, 2000.
17. **Luster AD and Ravetch JV.** Biochemical characterization of a gamma interferon-inducible cytokine (IP-10). *J Exp Med* 166: 1084–1097, 1987.
18. **Luster AD.** Chemokines-chemotactic cytokines that mediate inflammation. *N Engl J Med* 338: 436–445, 1998.
19. **Mosier DE, Yetter RA, and Morse HC 3rd.** Retroviral induction of acute lymphoproliferative disease and profound immunosuppresion in adult C57BL/6 mice. *J Exp Med* 161: 766–784, 1985.
20. **Narumi S, Kaburaki T, Yoneyama H, Iwamura H, Kobayashi Y, and Matsushima K.** Neutralization of IFN-inducible protein10/CXCL10 exacerbates experimental autoimmune encephalomyelitis. *Eur J Immunol* 32: 1784–1791, 2002.
21. **Narumi S, Tominaga Y, and Tamaru M.** Expression of IFN-inducible protein 10 in chronic hepatitis. *J Immunol* 158: 5536–5544, 1998.
22. **Ogawa N, Ping L, Zhenjun L, Takada Y, and Sugai S.** Involvement of the interferon-γ-induced T cell-attracting chemokines, interferon-γ-inducible 10-kd protein (CXCL10) and monokine induced by interferon-γ (CXCL9), in the salivary gland lesions of patients with Sjögren's syndrome. *Arthritis Rheum* 46: 2730–2741, 2002.
23. **Qin S, Rottman JB, Myers P, Kassam N, Weinblatt M, Loetscher M, Koch AE, Moser B, and Mackay CR.** The chemokine receptors CXCR3 and CCR5 mark subsets of T cells associated with certain inflammatory reactions. *J Clin Invest* 101: 746–754, 1998.
24. **Qu WM, Miyazaki T, Terada M, Okada K, Mori S, Kanno H, and Nose M.** novel autoimmune pancreatitis model in MRL mice treated with polyinosinic:polycytidylic acid. *Clin Exp Immunol* 129: 27–34, 2002.
25. **Romagnani S.** The Th1/Th2 paradigm. *Immunol Today* 18: 263–266, 1997.
26. **Sallusto F, Lanzavecchia A, and Mackay CR.** Chemokines and chemokine receptors in T-cell priming and Th1/Th2-mediated responses. *Immunol Today* 19: 568–574, 1998.
27. **Sasaki S, Yoneyama H, Suzuki K, Suriki H, Aiba T, Watanabe S, Kawauchi Y, Kawachi H, Shimizu F, Matsushima K, Asakura H, and Narumi S.** Blockade of CXCL10 protects mice from acute colitis and enhances crypt cell survival. *Eur J Immunol* 32: 3197–3205, 2002.
28. **Saurer L, Reber P, Schaffner T, Buchler MW, Buri C, Kappeler A, Walz A, Friess H, and Mueller C.** Differential expression of chemokines in normal pancreas and in chronic pancreatitis. *Gastroenterology* 118: 356–367, 2000.
29. **Singh UP, Singh S, Taub DD, and Lillard JW Jr.** Inhibition of IFN-γ-inducible protein-10 abrogates colitis in IL-10−/− mice. *J Immunol* 171: 1401–1406, 2003.
30. **Sorensen TL, Tani M, Jensen J, Pierce V, Lucchinetti C, Folcik VA, Qin S, Rottman J, Sellebjerg F, Strieter RM, Frederiksen JL, and Ransohoff RM.** Expression of specific chemokines and chemokine receptors in the central nervous system of multiple sclerosis patients. *J Clin Invest* 103: 807–815, 1999.
31. **Sorensen TL, Trebst C, Kivisakk P, Klaege KL, Majmudar A, Ravid R, Lassmann H, Olsen DB, Strieter RM, Ransohoff RM, and Sellebjerg F.** Multiple sclerosis: a study of CXCL10 and CXCR3 co-localization in the inflamed central nervous system. *J Neuroimmunol* 127: 59–68, 2002.
32. **Suzuki K, Fujiwara M, and Mizuochi T.** Exocrinopathy resembling Sjoegren's syndrome induced by a murine retrovirus: implication for a new animal model. In: *Sjoegren's Syndrome: State of the Art*, edited by Homma M, Sugai S, and Tojo T. Amsterdam: Kugler, 1994, p.171–173.
33. **Suzuki K, Makino M, Okada Y, Kinoshita J, Yui R, Kanazawa H, Asakura H, Fujiwara M, Mizuochi T, and Komuro K.** Exocrinopathy resembling Sjoegren's syndrome induced by a murine retrovirus. *Lab Invest* 69: 430–435, 1993.
34. **Uguccioni M, Gionchetti P, Robbiani DF, Rizzello F, Peruzzo S, Campieri M, and Baggiolini M.** Increased expression of IP-10, IL-8, MCP-1, and MCP-3 in ulcerative colitis. *Am J Pathol* 155: 331–336, 1999.
35. **Watanabe S, Suzuki K, Kawauchi Y, Yamagiwa S, Yoneyama H, Kawachi H, Okada Y, Shimizu F, Asakura H, and Aoyagi Y.** Kinetic analysis of the development of pancreatic lesions in mice infected with a murine retrovirus. *Clin Immunol* 109: 212–223, 2003.
36. **Yoneyama H, Narumi S, Zhang Y, Murai M, Baggiolini M, Lanzavecchia A, Ichida T, Asakura H, and Matsushima K.** Pivotal role of dendritic cell-derived CXCL10 in the retention of T helper cell 1 lymphocytes in secondary lymph nodes. *J Exp Med* 195: 1257–1266, 2002.

Original Paper

Absence of Pretreatment Markers that Predict the Emergence of YMDD Mutants during Lamivudine Treatment - The Results of a Prospective Multi-center Study

Masahiko Yano[1], Shogo Ohkoshi[1], Kenta Suzuki[1], Shin-ichi Ito[2], Hiroto Wakabayashi[2]
Motoya Sugiyama[3], Toshiaki Watanabe[4], Hironobu Maeda[5], Shige-aki Hatakeyama[6]
Tohru Hatano[7], Yuka Kobayashi[8], Shin-ichi Takei[9], Kohjiro Hata[10]
Yasunori Tsuboi[11], Tohru Takahashi[12], Tohru Ishikawa[13], Tomoteru Kamimura[13]
Takafumi Ichida[1], Yutaka Aoyagi[1]

[1]Gastroenterology Division, Graduate School of Niigata University, [2]Takeda General Hospital
[3]Ken-ritsu Sakamachi Hospital, [4]Sanjyo-Saiseikai Hospital, [5]Maeda Clinic, [6]Hatakeyama Clinic
[7]Nagaoka Chu-oh Hospital, [8]Tachikawa General Hospital, [9]Kariwagun General Hospital
[10]Niigata Municipal Hospital, [11]Internal Medicine of Nihon Dental University
[12]Nagaoka Red Cross Hospital, [13]Saiseikai II Hospital, Japan
Corresponding Author: Shogo Ohkoshi, MD, Division of Gastroenterology
Graduate School of Niigata University, 1-754 Asahimachi-Dori, Niigata-City 951-8122, Japan
Tel: +81 252272204, Fax: +81 252270776, E-mail: okoshi@med.niigata-u.ac.jp

KEY WORDS:
Lamivudine; YMDD mutant; Chronic hepatitis B; Mutant prediction

ABBREVIATIONS:
Lamivudine (LAM); Alanine Aminotransferase (ALT); Precore (Pre-C); Core Promoter (CP); Hepatitis B Virus (HBV)

ABSTRACT

Background/Aims: The emergence of YMDD mutants in patients who are treated with lamivudine may determine the clinical prognosis. However, currently there are no clinical or virological factors that predict specifically the emergence of the mutants.

Methodology: To define these factors, we analyzed 69 patients with chronic hepatitis B infection who were treated with lamivudine (LAM) and followed prospectively for at least 12 months.

Results: Of the 69 patients, 12 (17.4%) developed YMDD mutants up to 12 months after the start of LAM. The incidence of YMDD mutants was slightly higher in those who were younger, had higher HBV DNA titers, lower ALT levels, genotype C, and mutations in the core promoter before treatment. However, we could not find any significant factors that correlated with the appearance of the mutants.

Conclusions: Currently, using conventional virological assays, it is difficult to predict the development of mutants before LAM treatment. Management of flare-ups of hepatitis, due to the appearance of mutants, should always be envisaged when LAM treatment is started.

INTRODUCTION

Lamivudine (2', 3'-dideoxy-3'-thiacytidine) (LAM), a deoxycytidine analogue, has been shown to be effective in inhibiting hepatitis B virus (HBV) replication (1-3). A significant improvement in necroinflammatory activity following LAM treatment has also been shown (4,5). However, deterioration of the clinical course results from the emergence of YMDD mutants during treatment (6,7). This may cause an acute flare of alanine aminotransferase (ALT), probably due to the lysis of infected hepatocytes in the immune response to the newly developed variants, and even can result in decompensation of the liver disease (8-10). The management of the flare-up of hepatitis due to the mutants remains a controversial issue (11) and it is important to identify the pretreatment clinical and virological parameters that may predict the emergence of mutants.

The relationship between naturally occurring mutations in the HBV genome and the clinical course of HBV infection is an important topic for investigation. In particular, it is well known that a point mutation in the precore (Pre-C) region (nt 1896) abrogates the production of HBeAg and is closely associated with seroconversion to anti-HBe (12). Other important mutations reside in the core promoter (CP) of the genome (nt 1762 and 1764) and may regulate the synthesis of the pregenome mRNA and Pre-C mRNA (13). These mutations may affect the replication ability of HBV and induce a different level of immune response. They may be involved in disease progression and severity (14,15). Another clinical aspect that depends upon genetic diversity of HBV is the effect of HBV genotype (16). Significant findings regarding the relationship between genotype and progression of chronic HBV infection are accumulating (17).

Currently, detection of these mutations is readily available using routine laboratory tests (18,19). We

Hepato-Gastroenterology 2006; 53:124-127

therefore tried to use these parameters to clarify several issues regarding LAM treatment, particularly focusing on the prediction of the emergence of YMDD mutants during treatment.

METHODOLOGY

Sixty-nine patients with chronic hepatitis B or liver cirrhosis type B were enrolled at Niigata University Hospital and 13 affiliated Hospitals and followed prospectively. They were treated with LAM for at least 12 months. The clinical characteristics of the patients are shown in **Table 1**. All the patients were positive for HBsAg and negative for both anti-HCV and anti-HIV. Their mean age was 45.3 years and 55 (79.7%) patients were male. Forty-two (60.9%) were positive for HBeAg and 88% for genotype C HBV. Forty-eight (70%) were evaluated by liver biopsy.

Thirteen (19%) patients were diagnosed with liver cirrhosis. Of them, five were proven histologically and the other eight were diagnosed by the findings of both portal hypertension and hypoalbuminemia (<3.5g/dL).

The mean treatment period was 21.8 months and the maximum period was 86 months. Treatment was stopped in 22 (31.9%) patients, because of achievement of undetectable HBV DNA and normalization of ALT values in 15, appearance of YMDD mutants in 5, and development of multiple HCC and loss to follow-up each in one patient.

The histological findings in liver biopsy specimens were scored according to the classification of Desmet *et al.* (20). The stage of fibrosis was assessed from stage F0 (no fibrosis) to stage F4 (cirrhosis), and the grade of inflammatory activity was scored from grade A1 (mild) to grade A3 (severe).

HBeAg/anti-HBe was determined by enzyme immunoassays (Abbott Diagnostics, Chicago, IL). HBV genotype was determined by immunoassay based on genotype specific epitopes in the preS2 antigen (Genome Science Laboratory, Japan) (18). HBV DNA was examined by the transcription-mediated amplification (TMA) test (21). YMDD mutants were detected by a mini-sequencing method (Genome Science Laboratory, Japan) (19) and were confirmed by INNO-LiPA HBV DR (Innogenetics, NV, Belgium) (22). Precore (Pre-C) (nt 1896G to A) and core promoter (CP) (nt 1762A to T, 1764G to A) mutations were detected by the mini-sequencing method and a specific probe method (Genome Science Laboratory, Japan).

The Pre-C and CP region of the HBV genome was amplified and sequenced directly in five serum samples, which were chosen randomly. Briefly, DNA extracted from 50μL of serum was amplified by nested polymerase chain reaction using 5μL of resuspended DNA in a final volume of 25μL containing 0.3mM dNTP, 1M of each sense and antisense primers, and 0.6U Taq polymerase (Promega, Madison, WI). The external primers were 5'-CATAAGAGGACTCTTGGACT-3' (sense, nt 1,653 to 1672 of HBV genome) and 5'GGCGAGGGAGTTCTTCTTCTAGGGG-3' (antisense, nt 2,394 to 2,369), and primers for the second PCR were 5'-AATGTCAACGACCGACCTTG-3' (sense, nt 1,679 to 1698) and 5'-AGCTGAGGCGGTGTCGAGGAGATC-3' (antisense, nt 1,985 to 2,009). The reaction was performed for 35 cycles of 94°C 1 minute, 55°C 45 seconds, 72°C 1 minute. Direct sequencing was performed using an ABI DNA sequencer. The results obtained were consistent with the mutation pattern obtained by the kit in all the five samples.

The protocol for the research project has been approved by the Ethics Committees of the institution within which the work was undertaken. All the patients were given informed consent and patient anonymity was preserved.

Statistical Analysis

Mean age, ALT values, and HBV DNA titers were expressed as mean±SD. Comparisons of the incidence of Pre-C and CP mutations between the HBeAg(+) and HBeAg(-) patients were assessed by chi-square tests **(Table 2)**. The background clinical and virological factors of the patients who developed YMDD mutants and who did not were compared by Student's *t*-tests or chi-square **(Table 3)**. A p value less than 0.05 was considered statistically significant.

RESULTS

Pretreatment Pre-C, CP mutations, and HBV genotype were determined in 57 (82.6%), 50 (72.5%), and 67 (97.1%) of the 69 patients. Normalization of ALT values (≤40 IU/L) and undetectable HBV DNA titers (<3.7 LGE/mL) were obtained in 76.1% and 71.2% of the patients, respectively, after 12 months of treatment. Twelve (17.4%) of the 69 patients developed YMDD mutants within 12 months, and 17 (24.6%) developed them beyond this period. In total, 29 (42.0%) of the 69 patients developed mutants during treatment. All the 29 patients who developed mutants experienced an elevation of HBV DNA titer and 18 (62.1%) of the 29 showed an upsurge in ALT values (≥81). Mutant development within 12 months

TABLE 1 Clinical Characteristics of the Patients

Male:Female	55:14 (79.7%:20.3%)
Mean Age	45.3 (24?69)
HBV carrier in the family	30/63 (47.6%)
F factor	1:13:22:7:5(n=48)
F0:1:2:3:4	(2%:27%:46%:15%:10%)
HBeAg (+):(-)	42:27 (60.9%:39.1%)
HBV genotype B:C	8:59 (11.9%:88.1%)

TABLE 2 Relationship between HBeAg Status and Pretreatment PreC or CP Mutation

	Precore Mutant(-)	Precore Mutant(+)		CP Mutant(-)	CP Mutant(+)	
HBeAg(+)	29 (85.3%)	5 (14.7%)		6 (21.4%)	22 (78.6%)	
HBeAg(-)	7 (30.4%)	16 (69.6%)	$p<0.0001$	7 (31.8%)	15 (68.2%)	$p=0.5204$

TABLE 3. A Comparison of Clinical and Virological Factors between the Patients who Developed YMDD Mutants and Those who Did Not

	Mutant(+)	Mutant(-)	*p* value
Age	42.5±11.9	45.9±12.1	p=0.3700
ALT	160.2±119.3	226.0±271.4	p=0.4156
Sex M:F	10:2	45:12	p=0.7313
HBV DNA(-) after 3 months of LMV treatment	3/7 (42.9%)	32/45 (71.1%)	p=0.1382
Family history of HBV infection (+)/total	6/10 (60.0%)	24/53 (45.2%)	p=0.3927
HBeAg(+)/total	8/12 (66.7%)	34/57 (59.6%)	p=0.6507
HBV DNA(LGE)	7.38±1.20	7.14±1.33	p=0.5711
PreC mutation Mutant/All	5/12 (41.7%)	16/45 (35.6%)	p=0.6966
Core promoter Mutant/All	9/10 (90.0%)	28/40 (70.0%)	p=0.1972
Genotype B:C	0:12	8:47	p=0.1592
F factor (F0:1:2:3:4)	0:3:5:0:1	1:10:17:7:4	p=0.6918

of treatment had a probable association with an elevation of ALT (≥41) (p=0.0051) and a significant association with detectable HBV DNA (p=0020).

The relationship between Pre-C and CP mutations and HBeAg status is shown in **Table 2**. The incidence of Pre-C mutant (1896G to A) was significantly higher in the HBeAg-negative patients than in those positive for HBeAg [16/23 (69.6%) *vs.* 5/35 (14.3%), $p<0.0001$].

We compared the clinical and virological background factors between the patients who developed YMDD mutants within 12 months of the start of LAM (n=12, 17.4%) and those who did not (n=57, 82.6%) **(Table 3)**. Mean ALT values and HBV DNA titers were respectively lower and higher in the mutant (+) group, but this was not significant (p=0.4156 and p=0.5711, respectively). The frequency of the Pre-C mutant and CP mutations was higher in the mutant (+) group (41.7% *vs.* 34.8% for Pre-C, p=6966 and 90.0% *vs.* 70.0% for CP, p=0.1972). Genotype B was observed less frequently in the mutant (+) group than genotype C (0% *vs.* 14.5%, p=0.1592). A factor that was most likely to be associated with the development of the mutant was the incidence was positivity for HBV DNA after 3 months of treatment (57.1% in the mutant (+) group *vs.* 28.9% in the mutant (-) group, p=0.1382). However, these tendencies were not statistically significant.

DISCUSSION

The emergence of YMDD mutants is the sole factor that determines the clinical prognosis of patients treated with LAM (6,7). It is clearly associated with a breakthrough of hepatitis due to the reappearance of HBV DNA and can even result in hepatic decompensation (8-10). The clinical management of breakthrough hepatitis may be cumbersome and is still in debate. In contrast, the clinical course that goes without this mutation may be favorable. Therefore, our primary aim in this study was to seek virological and clinical factors that were associated with the development of the YMDD mutants. Physicians in this study were not asked to adhere to a particular treatment period and treatments were terminated after 12 to 24 months in a relatively large number of the patients. Therefore, we focused our analysis, especially prediction of mutant development, on the patients who were treated with LAM for at least 12 months and the analyses were targeted at the time point of 12 months after the start of the treatment.

The effects of LAM treatment, in terms of the rate of normalization of ALT and undetectable HBV DNA, were comparable to previous studies (3-5). Normalization of ALT values and undetectable HBV DNA titers were associated closely with a lack of appearance of mutants (p=0.0051, p=0.0020, respectively). Thus, effectiveness of LAM is determined by the appearance of mutants. So far, several reports discussed background characteristics that are associated with the appearance of YMDD mutants. Pretreatment high HBV DNA and ALT levels were shown to be factors associated with the emergence of YMDD mutants (23,24). Although there was a tendency for the development of mutants in patients with higher levels of HBV DNA, patients with higher ALT values had a lower incidence of mutants in this study. Pretreatment ALT values and HBV DNA titers do not seem to be definite predictors of the mutants. We also could not give a significant value to the severity of histological findings for the development of mutants.

The Pre-C mutant is known to be a good indicator of an HBeAg-negative state and a close association was found in this study **(Table 2)**. Because HBeAg-status may not be a good predictor of mutant development, this mutation also may not be able to forecast it. The CP mutations may reflect the stage of chronic liver disease due to HBV infection. These also are related to the progression of liver disease (17). There have been few reports concerning these mutations and their relation to the emergence of YMDD mutations. Because it became conventional to assay for these mutations in clinical laboratory investigations, we sought to determine whether these mutations could be a good predictor of clinical course during LAM treatment. We noticed that 74% (37/50) of the patients enrolled in this study already harbored these mutations. Although there was a slight tendency for the patients with these mutations to develop YMDD mutations, and correlated with abnormal ALT values, they may not to be a reliable marker for the prediction of YMDD mutants during LAM treatment. The emergence rate of LAM resistance may be independent of genotype B and C (25). In our study, in genotype B, although the number of the patients was small, the emergence rate of mutant was lower than those with genotype C. Judgment after a shorter treatment period (12 months) in our study might explain the discrepancy. Further large-scale study is needed to conclude this issue.

In conclusion, we could not give any significant values to clinical or virological markers that are conventionally available in the clinical laboratory, for the prediction of the emergence of YMDD mutants during LAM treatment. The effectiveness of LAM, its safety,

and a high compliance are now generally accepted. Although clinical criteria to use this drug have not been well defined, we always see some clinical situations where we need to use this drug. We are now waiting for the routine availability of other nucleoside analogs, such as adefovir dipivoxil and entecavir, that may effectively suppress the replication of YMDD mutants (11). The most effective anti-HBV strategy with multiple drug use including interferon that stimulates endogenous immunity should be elucidated in future.

ACKNOWLEDGEMENT

This work was partially supported by a grant from GlaxoSmithKline, Japan. The authors thank Ms Naomi Cho for technical assistance.

REFERENCES

1 **Doong SL, Tsai CH, Schinazi RF, Liotta DC, Cheng YC:** Inhibition of the replication of hepatitis B virus in vitro by 2', 3'-dideoxy-3'-thiacytidine and related analogues. Proc Natl Acad Sci USA 1991; 88:8495-8499.

2 **Chang CN, Doong SL, Zhou JH, Beach JW, Jeong LS, Chu CK, et al:** Deoxycitidine deaminase-resistant stereoisomer is the active form of (+/-)-2', 3' dideoxy-3'-thiacytidine in the inhibition of hepatitis B virus replication. J Biol Chem 1992; 267:13938-13942.

3 **Dienstag JL, Perrillo RP, Schiff ER, Bartholomew M, Vicary C, Rubin M:** A preliminary trial of lamivudine for chronic hepatitis B infection. N Engl J Med 1995; 333:1657-1661.

4 **Lai CL, Chien RN, Leung NW, Chang TT, Guan R, Tai DI, et al:** A one year trial of lamivudine for chronic hepatitis B infection. Asia Hepatitis Lamivudine Study Group. N Engl J Med 1998; 339:61-68.

5 **Dienstag JL, Schiff ER, Wright TL, Perrillo RP, Hann HW, Goodman Z, et al:** Lamivudine as initial treatment for chronic hepatitis B in the United States. N Engl J Med 1999; 341:1256-1263.

6 **Allen MI, Deslauriers M, Andrews CW, Tipples GA, Walters KA, Tyrrell DL, et al:** Identification and characterization of mutations in hepatitis B virus resistant to lamivudine. Lamivudine Clinical Investigation Group. Hepatology 1998; 27:1670-1677.

7 **Buti M, Jardi R, Cotrina M, Rodriguez-Frias F, Esteban R, Guardia J:** Transient emergence of hepatitis B variants in a patient with chronic hepatitis B resistant to lamivudine. J Hepatol 1998; 28:510-513.

8 **Liaw Y-F, Chien R-N, Yeh C-T, Tsai S-L, Chu C-M:** Acute exacerbation and hepatitis B virus clearance after emergence of YMDD motif mutation during lamivudine therapy. Hepatology 1990; 30:567-572.

9 **Bruno R, Sacchi P, Malfitano A, Filice G:** YMDD-mutant HBV strain as a cause of liver failure in an HIV-infected patient. Gastroenterology 2001; 121:1027-1028.

10 **Bessesen M, Ives D, Condreay L, Lawrence S, Sherman KE:** Chronic active hepatitis B exacerbations in human immunodeficiency virus-infected patients following development of resistance to or withdrawal of lamivudine. Clin Infect Dis 1999; 28:1032-1035.

11 **Liaw YF:** Management of YMDD mutations during lamivudine therapy in patients with chronic hepatitis B. J Gastroenterol Hepatol 2002; Suppl 3:S333-S337.

12 **Hadziyannis SJ, Vassilopoulos D:** Hepatitis B e antigen-negative chronic hepatitis B. Hepatology 2001; 34:617-623.

13 **Kramvis A, Kew MC:** The core promoter of hepatitis B virus. J Viral Hepat 1999; 6:415-427.

14 **Takahashi K, Aoyama K, Ohno N, Iwata K, Akahane Y, Baba K, et al:** The precore/core promoter mutation of hepatitis B virus: clinical significance and an easy method of detection. J Gen Virol 1995; 75:3159-3164.

15 **Baumert TF, Rogers SA, Hasegawa K, Liang TJ:** Two core promoter mutations identified in a hepatitis B virus strain associated with fulminant hepatitis result in enhanced viral replication. J Clin Invest 1996; 98:2268-2276.

16 **Orito E, Mizokami M, Sakugawa H, Michitaka K, Ishikawa K, Ichida T, Okanoue T, Yotsuyanagi H, Iino S:** A case-control study for clinical and molecular biological differences between hepatitis B viruses of genotypes B and C. Japan HBV Genotype Research Group. Hepatology 2001; 33:218-223.

17 **Sumi H, Yokosuka O, Seki N, Arai M, Imazeki F, Kurihara T, et al:** Influence of hepatitis B virus genotypes on the progression of chronic type B liver disease. Hepatology 2003; 37:19-26.

18 **Usuda S, Okamoto H, Iwanari H, Baba K, Tsuda F, Miyakawa Y, et al:** Serological detection of hepatitis B virus genotypes by ELISA with monoclonal antibodies to type-specific epitopes in the preS2-region product. J Virol Methods 1999; 80:97-112.

19 **Kobayashi S, Shimada K, Suzuki H, Tanikawa K, Sata M:** Development of a new method for detecting a mutation in the gene encoding hepatitis B virus reverse transcriptase active site (YMDD) motif. Hepatol Res 2000; 17:31-42.

20 **Desmet VJ, Gerber M, Hoofnagle JH, Manns M, Sheuer PJ:** Classification of chronic hepatitis: diagnosis, grading and staging. Hepatology 1994; 19:1513-1520.

21 **Kamisango K, Kamogawa C, Sumi M, Goto S, Hirao A, Gonzales F, et al:** Quantitative detection of hepatitis B virus by transcription- mediated amplification and hybridization protection assay. J Clin Microbiol 1999; 37:310-314.

22 **Stuyver L, Van Geyt C, De Gendt S, Van Reybroeck G, Zoulim F, Leroux-Roels G, et al:** Line probe assay for monitoring drug resistance in hepatitis B virus- infected patients during lamivudine therapy. J Clin Microbiol 2000; 38:702-707.

23 **Yuen M-F, Sablon E, Hui C-K, Yuan H-J, Decraemer H, Lai C-L:** Factors associated with hepatitis B virus DNA breakthrough in patients receiving prolonged lamivudine therapy. Hepatology 2001; 34:785-791.

24 **Lai CL, Yuen MF:** Profound suppression of hepatitis B virus replication with lamivudine. J Med Virol 2000; 6:367-373.

25 **Akuta N, Suzuki F, Kobayashi M, Tsubota A, Suzuki Y, Hosaka T, et al:** The influence of hepatitis B virus genotype on the development of lamivudine resistance during long-term treatment. J Hepatol 2003; 38:315-321.

Laboratory Investigation (2006) 86, 687–696

www.laboratoryinvestigation.org

MEK/ERK signaling is a critical mediator for integrin-induced cell scattering in highly metastatic hepatocellular carcinoma cells

Nobuyuki Honma[1], Takuya Genda[1], Yasunobu Matsuda[1], Satoshi Yamagiwa[1], Masaaki Takamura[1], Takafumi Ichida[2] and Yutaka Aoyagi[1]

[1]*Division of Gastroenterology and Hepatology, Department of Cellular Function, Niigata University Graduate School of Medical and Dental Science, Niigata City, Japan and* [2]*Department of Gastroenterology, Juntendo University School of Medicine and Juntendo University Hospital of Shizuoka, Shizuoka, Japan*

The human hepatocellular carcinoma (HCC)-derived cell line KYN-2 is thought to provide a good model for studying the molecular basis of invasion and metastasis of human HCC, because it often shows cell scattering *in vitro* and intrahepatic metastasis *in vivo*. We previously found that integrin-mediated extracellular signals inactivated E-cadherin in KYN-2, and caused loss of cell–cell contact with gain of cell motility, which is considered to be a critical step in the process of cancer cell invasion and metastasis. To further understand molecular mechanisms involved in biological aggressiveness of HCC, we investigated intracellular signaling involved in integrin-mediated scattering of KYN-2 cells. Cultured KYN-2 cells formed trabecular aggregates in suspension, but when adhering to integrin-stimulating substrata, they scattered according to phosphorylation of extracellular signal-regulated kinase (ERK). Upon treatment with ERK kinase (MEK) inhibitor PD98059, adhered KYN-2 cell scattering was inhibited, tight cell-to-cell contact was recovered, and both E-cadherin and actin filaments accumulated in the area of intercellular contact zone. In contrast, constitutively active MEK1-transfected KYN-2 cells showed reduced E-cadherin and actin filaments in the intercellular contact zone, showing a flattened phenotype with broad lamellipodia. Enforced signaling of MEK-ERK pathway in KYN-2 cells suppressed cadherin-mediated homotypic adhesion and increased the potential of cell motility. An antibody-based protein microarray analysis revealed that the cytoplasmic protein c-Cbl was significantly downregulated in MEK1-transfected KYN-2 cells, suggesting that c-Cbl might be a candidate downstream mediator of integrin/MEK/ERK-mediated cell scattering. In conclusion, cell scattering of the highly metastatic cell line KYN-2 is regulated through the integrin-MEK-ERK signaling cascade, suggesting that this molecular pathway may be critical in intrahepatic metastasis of human HCC.
Laboratory Investigation (2006) **86,** 687–696. doi:10.1038/labinvest.3700427; published online 8 May 2006

Keywords: actin; c-Cbl; cell motility; E-cadherin; intrahepatic metastasis; liver cancer

Hepatocellular carcinoma (HCC) is one of the most aggressive malignancies found worldwide. Despite considerable progress in diagnostic and therapeutic modalities, prognosis of HCC remains poor, because it often reoccurs and spreads by metastasis within a short time.[1,2] HCC metastasis is mainly due to tumor cell dispersal to surrounding liver tissues through the portal vein,[3] a mechanism which is generally clinically referred to as 'intrahepatic metastasis'. Pathological studies have suggested that cancer cell scattering from the tumor periphery may be closely associated with intrahepatic metastasis of HCC,[4] but its biological significance is not fully understood. In a previous study, we injected various types of human hepatoma cell lines into the livers of SCID mice, and found that their scattering abilities *in vitro* strongly correlated with potential of intrahepatic metastasis.[5] When scattering ability of highly-metastatic hepatoma cell lines was inhibited by dominant-negative Rho-kinase or Rho-kinase inhibitors, significant loss in metastatic potential was observed.[5,6] Taken together, scattering ability of hepatoma cells *in vitro* might be tightly correlated with their metastatic ability *in vivo*, and investigation of molecular mechanisms of hepatoma cell scattering seems valuable for understanding the invasive phenotype of HCC.

Among hepatoma cell lines, the human HCC-derived cell line KYN-2 has been regarded as a good

Correspondence: Dr T Genda, MD, Division of Gastroenterology and Hepatology, Department of Cellular Function, Niigata University Graduate School of Medical and Dental Science, Asahimachi-dori 1-757, Niigata City 951-8510, Japan.
E-mail: tgenda@sbthp.jp
Received 4 October 2005; revised 13 March 2006; accepted 14 March 2006; published online 8 May 2006